Dielectric function for a disordered one-dimensional conductor*†

Robert L. Bush

Department of Physics and The James Franck Institute, The University of Chicago, Chicago, Illinois 60637 and Radiation Laboratory,§‖ University of Notre Dame, Notre Dame, Indiana 46556

(Received 2 June 1975)

We present a calculation of the wave vector and frequency dependence of the longitudinal dielectric function of a disordered material which is collection of noninteracting parallel chains. We used a one-dimensional tight-binding model with nearest-neighbor interaction only, and randomness in the diagonal elements of the Hamiltonian. The model does not contain electron-phonon interactions, and is therefore valid only at zero temperature. The dielectric function is calculated from integral equations after a method developed by Halperin. The graphs of ϵ_2 vs frequency resemble those for ϵ_2 (crystalline), but broadened by W/L, where W is the crystal bandwidth and L is the decay length of the wave functions in the random system. The graphs of ϵ_1 show a similar broadening. We find $\epsilon_1(\omega = 0) \approx 1 + 0.993\kappa^2[q^2 + 1.56/(Lb)^2]^{-1}$ (κ is the Fermi-Thomas screening factor, b is the lattice constant) for $qb \leq 0.2\pi$. The peak in the conductivity at zero wave vector occurs at a frequency which is inversely proportional to L. The disorder also removes the singularity in ϵ_1 at $q = 2k_F$, $\omega = 0$; the condition for a Peierls distortion in the presence of disorder is discussed. These results are interpreted in terms of the localized states in one-dimensional disordered systems.

I. INTRODUCTION

Recently certain classes of materials have been discovered which exhibit strong anisotropy, especially in their dc conductivity and optical properties. Two classes of particular interest are the mixed-valence planar complexes (MVPC) of platinum [e.g., $K_2Pt(CN)_4Br_{0.3} \cdot n H_2O$], [1,2] and compounds containing linear stacks of organic ion radicals such as the anion tetracyanoquinodimethane (henceforth TCNQ).[3,4] A wealth of experimental data has been amassed[5,6] for these systems, and several theories have been advanced which attempt to explain the data. Heeger and collaborators[6] have applied the Mott-Hubbard model to the compound N-methylphenaziniumTCNQ (NMP-TCNQ), and claim that it undergoes a transition from a metallic state to an antiferromagnetic insulating state at 215 K.[6] That is, above 215 K the conduction band is half full, but below that temperature the band is split into two by the Coulomb repulsion energy of two electrons on the same TCNQ molecule. To get the proper band splitting they require a polarizability of 100 Å^3 for the NMP ion. They claim that otherwise the splitting would be too large to fit the conductivity data.

Rice and Bernasconi have proposed a model for the MVPC materials in which disorder is provided by dislocations and impurities, leading to a picture of interrupted metallic strands.[7] They have also published a calculation of the dielectric function in this model,[8] which reproduces the large positive dielectric constant observed at low frequencies.[9]

In addition, Bloch, Weisman, and Varma (BWV) have proposed that many of these materials can be grouped together into a class of nearly one-dimensional disordered conductors.[10] They claim there is intrinsic disorder in many of the materials in addition to extrinsic disorder introduced by defects and impurities. For example, NMP$^+$ has a large electric dipole moment (about 1.1 D),[11] which can be oriented randomly in either of two opposite directions with equal probability.[12] [Recently new experimental evidence has been reported which calls into question this source of randomness. Kobayashi[13] reports x-ray diffraction data which indicate that the NMP dipoles alternate along the chains (a axis), and are all aligned parallel along the b axis, but there is no order in the third (c) direction. Morosin,[14] on the other hand, has x-ray diffraction data which show no such structure, but which are consistent with the BWV interpretation. Perhaps the difference in their results may be due to differences in sample preparation. Theodorou and Cohen[15] have compiled magnetic susceptibility data, which also show strong sample dependence.] The electrostatic potential produced by these randomly oriented dipoles will provide a random potential at the positions of the electrons. In the MVPC, the Br^- sites and the H_2O sites are partially and randomly occupied. (The K^+ occupy fixed positions according to recent x-ray[16] and neutron-diffraction[17] experiments, although they had previously been thought to be random.) The Br^- are charged, and H_2O has a large permanent electric dipole moment. Randomness in their configuration may produce a large random component in the potential felt by an electron moving in the Pt chains.

It is interesting to note that in both these cases the disorder potential is of electrostatic origin, and hence will be modified by any dielectric

screening which takes place in these materials. Moreover, it is of interest to establish just how much of their large dielectric constant is associated with the conduction electrons and how much with the molecular framework in which those electrons move.

It is in the light of these considerations that we have calculated the dielectric function $\epsilon(q, \omega)$ for a model of a disordered material which exhibits one-dimensional conductivity. Pollak has published a derivation of a dielectric function for an amorphous semiconductor, [18] which takes local fields into account, but which requires knowledge of the form of the wave functions for an application. Since we do not know the form of the wave functions, we are unable to use his results. The method used here avoids any need to calculate wave functions.

In Sec. II we report the results of a calculation which shows that the contribution of the bonding electrons and the ionic lattice to the dielectric constant is too small to account for observed values. Section III contains a description of the model we have chosen to represent conduction electrons in these materials, and the form the dielectric function of a one-dimensional system takes in the random-phase approximation (RPA). We suggest some simple approximate calculations of the dielectric function for random one-dimensional systems in Sec. IV. Section V describes the mathematical formalism for calculating the conduction-electron contribution to the dielectric function, and Sec. VI details the numerical aspects of the calculation. We report and discuss our numerical results in Sec. VII.

II. POLARIZABILITY OF BONDS AND IONS

The dielectric constants of several of these materials have been measured at microwave frequencies. That for $K_2Pt(CN)_4Br_{0.3}\cdot 2.3H_2O$ is about 10^3, as measured by Berenblyum *et al.* [9] That for NMP-TCNQ was measured by Buravov *et al.* [19] and was found to vary from about 350 at 4 K to about 800 at 80 K. Buravov *et al.* also measured the dielectric constant of acridinium-$(TCNQ)_2$, [19] and it was of the same order of magnitude.

We first asked whether polarization of the bonding electrons and the ions can account for the large dielectric constant of NMP-TCNQ. (A relatively small polarizability can produce a large dielectric constant if the geometry is right.) We took from the chemical literature[20–23] the polarizabilities of the interatomic bonds, and assigned half to each atom in the bond. The mean polarizability of neutral phenazine calculated in this way is 25.3 Å^3, in good agreement with the measured value, 23.4 Å^3, [24] and that calculated for NMP^+ is 27.2 Å^3, a factor of four too small to give the screening of intramolecular electron repulsion required by Epstein *et al.* [6] We calculated the effect of ionic motion by assuming that the molecules moved as rigid units in a simple harmonic oscillator potential, whose force constant was taken from the coefficient of T^3 in the low-temperature specific heat, [25] which has been measured by Etemad, Garito, and Heeger. [26] Further details of this calculation will be published elsewhere. [27] The results depend on the anisotropy of the ionic force constant, but for any of the values we chose, the eigenvalues of the dielectric tensor were all less than two, and one was slightly negative. These values are less than $\frac{1}{100}$ of the measured dielectric constant at microwave frequencies (which are nearly zero on the scale of any other frequencies in NMP-TCNQ). Moreover, the eigenvector corresponding to our negative eigenvalue is perpendicular to the chain axis, the direction of the large measured dielectric constant. Hence a model which assumes that all the electrons are localized on individual molecules cannot be used for the low-frequency dielectric properties of NMP-TCNQ. We now study a different model, one in which the conduction electron states, not yet considered by us, are localized by disorder not to within a molecule, but rather to a region of several molecules along the high-conductivity axis; the extension of the states being determined by their energy and the randomness in the system. [28–30]

III. MODEL

We choose as our model of a one-dimensional conductor a set of chains of sites or molecules. Along each chain the sites are separated by a distance b. The chains are assumed to be noninteracting; the transition probability for hopping between chains is taken to be zero. Each chain is further assumed to occupy an area A_c, which is defined by the relation $\Omega = NN_c bA_c$, where Ω is the volume of the system, N is the number of sites per chain, and N_c is the number of chains in the volume.

We represent each chain by a tight-binding Hamiltonian with diagonal randomness only

$$H = \sum_n \epsilon_n |n\rangle\langle n| + t\sum_n (|n\rangle\langle n+1| + |n+1\rangle\langle n|), \tag{3.1}$$

where t is the nearest-neighbor interaction, assumed constant (we shall choose the unit of energy in Sec. V so as to set $t=1$), and ϵ_n is a random diagonal site energy. The ϵ_n are independent random variables, each with a Gaussian distribution of width St. We shall refer to the quantity S as the "randomness." Each $|n\rangle$ is a wave function for an electron in a tight-binding orbital at site n. It can be shown that the dipolar contribution to the

randomness in the ϵ_n in NMP-TCNQ is approximately Gaussian in form.[31] In the absence of any screening,

$$S^2t^2 = d^2e^2\sum_l \cos^2\theta_l\, r_l^{-4}, \tag{3.2}$$

where d is the dipole moment of a NMP molecule (about 1.1 D), r_l is the distance from a particular TCNQ molecule to the lth NMP molecule, and θ_l is the angle between the dipole moment and $\vec{r}_l$ in the point dipole approximation. From Eq. (3.2) we find $St = 0.76$ eV. As the bandwidth in these materials is believed to be about 0.1 eV,[6] this randomness parameter would be much larger than the nearest-neighbor interaction t. If there was no screening, the electrons would be very tightly localized indeed and the conductivity would be smaller than observed. If we assume that the screening can be calculated with the aid of a simple functional form for the dielectric function, we can now solve the problem self-consistently: Find a dielectric constant which produces the proper random potential to reproduce itself.

We shall assume further that the tight-binding functions are sufficiently localized that we may approximate

$$\langle n|f(r)|n'\rangle = f(r_n)\,\delta_{nn'}, \tag{3.3}$$

where f is any function of distance along the chain. We see in Sec. V that the formalism by which we calculate the dielectric function requires this assumption.

We have omitted the electron-phonon interaction from the Hamiltonian (3.1); phonon-assisted hopping is thereby eliminated. The resulting dielectric function is correct only at $T=0$ or at frequencies larger than any important hopping rate. We shall comment in Sec. VII on the deviations from our results which are expected when these conditions are violated.

We have calculated the dielectric function in the random-phase approximation (RPA), in which the dielectric function takes the form[32]

$$\epsilon(q,\omega) = 1 - \lim_{\alpha\to 0^+}\frac{4\pi e^2}{q^2\Omega} \times \sum_{kk's}\frac{|\langle ks|e^{-i\vec{q}\cdot\vec{r}}|k's\rangle|^2[f(E_k)-f(E_{k'})]}{E_k - E_{k'} - \hbar\omega + i\hbar\alpha}. \tag{3.4}$$

Here k and k' are eigenstates of the Hamiltonian (and are not Bloch waves unless there is no randomness), s is the electron-spin coordinate, Ω is the volume of the system, and f is the Fermi distribution function. Since we are dealing with random systems, we are interested in an ensemble average of the dielectric function. Because we have assumed that the chains are independent of each other, each eigenstate is confined to a single chain, and the matrix elements linking states on different chains are zero. Localization of the eigenstates to single chains requires only that the randomness S be large compared to any interchain matrix element of H. Because of this independence, we may replace the index k with two indices i and j, where i is a (two-dimensional) chain index and j indexes the states within a chain. Then the double sum in (3.1) becomes a sum over i, i', j, and j'. The sum over i' may now be done trivially—only the terms with $i=i'$ contribute. The ensemble average of the sum over chains is simply the product of the number of chains N_c and the ensemble average of the sum j and j' on a single chain.

We then have

$$\langle\epsilon(q,\omega)\rangle = 1 - \lim_{\alpha\to 0^+}\frac{4\pi e^2}{q^2V_cN} \times\left\langle\sum_{jj's}\frac{|\langle js|e^{-i\vec{q}\cdot\vec{r}}|j's\rangle|^2[f(E_j)-f(E_{j'})]}{E_j - E_{j'} - \hbar\omega + i\hbar\alpha}\right\rangle, \tag{3.5}$$

where V_c is the volume of a unit cell, $V_c = A_cb$.

IV. SIMPLE MODELS OF THE DIELECTRIC FUNCTION

The primary feature of random one-dimensional systems which sets them off from their crystalline counterparts is the localization of the electronic wave functions. In this section we derive expressions for the dielectric function which take this localization into account. We shall compare these results with the results of our exact calculation in Sec. VII.

A. Imaginary part

Suppose the wave functions in the random system are like those in a crystalline system but decay exponentially on either side of a maximum,

$$|k\rangle = (Lb)^{-1/2}\exp(ikx - |x-x_k|/Lb), \tag{4.1}$$

where x_k is the center of state $|k\rangle$, assumed to vary randomly from state to state, and L, the exponential decay length, is assumed independent of k. Then we find

$$\langle k|e^{i\vec{q}\cdot\vec{r}}|k'\rangle = L^{-1}\exp[-|x_k - x_{k'}|/Lb + \tfrac{1}{2}i(k'+q-k)(x_k+x_{k'})]\,(\{[2/L + ib(k'+q-k)]^{-1} - [ib(k'+q-k)]^{-1}\} \times\exp[\tfrac{1}{2}i(k'+q-k)(x_k-x_{k'})] + \{[2/L - ib(k'+q-k)]^{-1} + [ib(k'+q-k)]^{-1}\}\exp[-\tfrac{1}{2}i(k'+q-k)(x_k-x_{k'})]). \tag{4.2}$$

On squaring and averaging over all possible values of $|x_k - x_{k'}|$, assuming that variable to be distributed uniformly in $[0, Nb]$, we obtain

$$|\langle k|e^{i\vec{q}\cdot\vec{r}}|k'\rangle|^2_{av} = N^{-1}\{\tfrac{1}{2}[1+\tfrac{1}{4}(k'+q-k)^2L^2b^2]^{-3} + \tfrac{3}{4}[1+\tfrac{1}{4}(k'+q-k)^2L^2b^2]^{-2}\}. \quad (4.3)$$

From Eq. (3.5) we have

$$\epsilon_2(q,\omega) = \frac{8\pi^2e^2}{q^2\Omega}\left(\frac{Nb}{2\pi}\right)^2\int dk\int dk'\,|\langle k|e^{i\vec{q}\cdot\vec{r}}|k'\rangle|^2_{av} \times[f(E_k)-f(E_{k'})]\,\delta(E_k-E_{k'}+\hbar\omega), \quad (4.4)$$

where we have replaced the sums with integrals. If we assume further that $\hbar\omega \ll 2t$, so that all quantities may be evaluated at the Fermi energy, and that $E(k)\approx 2tb(k_F-k)$ as it does in the crystal, then

$$\epsilon_2(q,\omega) = [4\pi^2e^2Ln^2(E_F)\hbar\omega/q^2V_c] \times(\tfrac{1}{2}D^{-3}+\tfrac{3}{4}D^{-2}), \quad (4.5)$$

where $n(E_F)$ is the density of states per site at the Fermi level and D is given by

$$D = 1+\tfrac{1}{4}(qb-\hbar\omega/2t)^2L^2. \quad (4.6)$$

Note that $\epsilon_2(q,\omega)$ is linear in frequency for low frequency. At higher frequencies the function D dominates the dependence. It provides a maximum in ϵ_2 at $\hbar\omega = 2qbt$, with a width of $4t/L$.

The small q behavior of Eq. (4.5) is clearly incorrect for disordered systems. As $q\to 0$, Eq. (4.5) predicts $\epsilon_2 \to 1/q^2$. The reason lies in the approximation of the wave functions of the random system by Eq. (4.1). This expression implies more phase coherence than is actually present in random systems, and as a result overestimates matrix elements. For example, $\langle k|k'\rangle \neq \delta_{kk'}$ since the exponential factor prevents the $e^{i(k-k')x}$ factor from averaging to zero. For small q,

$$\langle k|e^{i\vec{q}\cdot\vec{r}}|k'\rangle \approx \langle k|k'\rangle + i\vec{q}\cdot\langle k|\vec{r}|k'\rangle.$$

If the first term does not vanish, there will be an erroneous $1/q^2$ contribution to the dielectric function. At large q, we might also expect this expression to be invalid at large frequency, because of the approximations made in the sentence before Eq. (4.5).

B. Real part

The real part of the dielectric function may be obtained from the imaginary part by Kramers-Kronig analysis. If we use Eq. (4.5) to calculate $\epsilon_1(q,0)$, we obtain

$$\epsilon_1(q,0) = 1+[4e^2n(E_F)/q^2V_c][\tfrac{1}{2}\pi+3+\tan^{-1}\tfrac{1}{2}qLb + \tfrac{1}{2}qL/(1+\tfrac{1}{4}q^2L^2)+\tfrac{3}{2}qL/(1+\tfrac{1}{4}q^2L^2)^{1/2}]. \quad (4.7)$$

In the limit $L\to\infty$, which corresponds to a perfect crystal, Eq. (4.7) reproduces the proper dependence on q for low q, but is a factor of 1.5 too large. For finite L, and small wave vector, Eq. (4.7) suffers from the same limitations as Eq. (4.5)—the nonorthogonality of the wave functions provides a spurious term proportional to $1/q^2$. Equation (4.7) does not reproduce the Peierls singularity at $q = 2k_F$. This occurs because it is an integral over frequency of Eq. (4.5), whose validity is restricted to low frequencies. For wave vectors near $2k_F$ the important contributions to ϵ_2 cover a wide frequency range. As much of this range is not adequately described by Eq. (4.5), we do not expect Eq. (4.7) to be accurate either.

A simpler expression for $\epsilon_1(0,0)$ may be obtained from the following argument:

$$\epsilon_1(0,0) = 1+\frac{8\pi e^2}{\Omega}\sum_{kk'}|\langle k|x|k'\rangle|^2 \times[f(E_k)-f(E_{k'})](E_{k'}-E_k)^{-1}. \quad (4.8)$$

Assume that $\langle k|x|k'\rangle = Lb$ if $|k-k'|\le 1/Lb$ and if $|x_k - x_{k'}|\le Lb$, and $\langle k|x|k'\rangle = 0$ otherwise. That is, the matrix element will be zero unless both wave functions are appreciable in the same region of space, and at the same time close enough together in wave vector that they will stay in phase over their entire length (otherwise the oscillations will cause the matrix element to vanish). We replace the sums by integrals giving

$$\epsilon_1(0,0) = 1+4\frac{8\pi e^2}{\Omega}\left(\frac{Nb}{2\pi}\right)^2\int_{k_F-1/Lb}^{k_F}dk \times\int_{k_F}^{k_F+1/Lb}dk'\,\frac{2L}{N}(Lb)^2(E_k-E_{k'})^{-1}, \quad (4.9)$$

where the factor of 4 comes from the four equivalent regions of the Brillouin zone which contribute, and the $2L/N$ arises from an average over the (uniformly distributed) $|x_k - x_{k'}|$. Set $E_k - E_{k'} = 2tb(k'-k)$, which should be valid for states near the Fermi level. With these changes Eq. (4.9) becomes

$$\epsilon_1(0,0) = 1+8\pi e^2(Lb)^3(V_c\pi^2t)^{-1}\int_{k_F-1/Lb}^{k_F}dk \times\int_{k_F}^{k_F+1/Lb}dk'\,(k'-k)^{-1} = 1+\frac{2\kappa^2(Lb)^2}{\pi}, \quad (4.10)$$

where κ is the inverse of the Thomas-Fermi screening length, $\kappa^2 = 8\pi e^2n(E_F)/V_c$.

To generalize to finite wave vectors, we observe that for a metal, for which $L=\infty$,

$$\epsilon_1(q,0) = 1+\kappa^2/q^2. \quad (4.11)$$

Then a disordered system might be expected to have a dielectric function of the form

$$\epsilon_1^A(q,0)=1+\kappa^2[q^2+\pi/2(Lb)^2]^{-1}. \quad (4.12)$$

We see that Eq. (4.12) reduces to Eq. (4.11) if $L\to\infty$, and to Eq. (4.10) if $q\to 0$.

If we write $\epsilon_1=1+4\pi\alpha/V_c$, where α is the polarizability of an electron, we observe from Eq. (4.10) that $\alpha\propto(Lb)^2$. A similar result has been reported by Berezinskii,[33] although his numerical factors are considerably larger than ours. We attribute the difference to the fact that our calculation is not done in the weak-scattering limit or near the band edge as, in effect, his was.

C. Conductivity

There are three distinct frequency regions in which the conductivity $\sigma(q,\omega)=\omega\epsilon_2(q,\omega)/4\pi$ shows qualitatively different behavior. They are a low-frequency region, where it is proportional to ω^2, a peak at about $\pi t/L$, and a Drude-like tail at high frequencies.

For finite wave vector, the quadratic frequency dependence follows directly from Eq. (4.5). For $q=0$, an argument similar to that for ϵ_1 gives quadratic dependence for σ. (A similar argument is given in Mott and Davis.[34]) The basic expression for the conductivity is

$$\sigma(\omega)=\frac{\omega}{4\pi}\frac{8\pi^2e^2}{\Omega}\sum_{kk'}|\langle k|x|k'\rangle|^2 \times[f(E_k)-f(E_{k'})]\,\delta(E_k-E_{k'}+\hbar\omega). \quad (4.13)$$

Under the same assumptions about matrix elements and energy dispersion that we made above, Eq. (4.13) becomes

$$\sigma(\omega)=\frac{2\pi e^2}{\hbar\Omega}2\hbar\omega\left(\frac{Nb}{2\pi}\right)^2\int_{k_F}^{k_F+\hbar\omega/2tb}dk\int_0^{k_F}dk'(Lb)^2\frac{2L}{N}(2tb)^{-1}\delta\left(k-k'+\frac{\hbar\omega}{2tb}\right)$$
$$=\frac{2\pi e^2}{\hbar V_c}\hbar\omega\frac{b}{2\pi^2t}L^3b^2\int_{k_F}^{k_F+\hbar\omega/2tb}dk=\frac{2\pi e^2}{\hbar V_c}n^2(E_F)L^3b^2(\hbar\omega)^2. \quad (4.14)$$

This expression is valid only for low frequencies, and is surely invalid if $\hbar\omega/2t\geq 1/L$, since the cancellation in matrix elements which restricted the integrals in Eq. (4.10) has not been taken into account.

Berezinskii[33] has recently reported a calculation of the conductivity which shows $\sigma\propto\omega^2\ln^2(\omega/\omega_0)$; our calculation is not sufficiently sensitive to note the difference between ω^2 and $(\omega\ln\omega)^2$. There may be quantitative differences between his prefactors and ours, but they agree qualitatively; we attribute the difference to the difference in the models: he is working in the weak-scattering band-edge limit, while we are not.

The conductivity should peak when the Fermi-level electrons are in resonance with the perturbing field. If the electron is thought of as a particle bounding back and forth with velocity v_F in a box of length $2Lb$ (one decay length on either side of a maximum), it would be in resonance with a field of frequency $\nu=v_F/4Lb$. Translated into energy units this becomes

$$\hbar\omega=\pi t/L. \quad (4.15)$$

On the high-frequency end Eq. (4.5) predicts $\sigma\propto\omega^{-2}$, like the result of the Drude theory, $\sigma(\omega)=\omega_p^2/(4\pi\tau\omega^2)$. For this system Eq. (4.5) implies $\tau=\pi\hbar L/16t=\pi Lb/8v_F$, i.e., the mean free path at optical frequencies Λ_{opt} in this system is $\Lambda_{opt}=\frac{1}{8}\pi Lb=0.39Lb$. [But it should be noted that Eq. (4.5) was derived under the assumption that ω was small, so these numerical factors ought not be taken too seriously.] We may, however, construct a dc mean free path Λ_{dc} by the following argument.

The reciprocal of the mean free path is the mean probability of scattering per unit length. An electron at the center of a tight-binding band which is periodic except that one site energy is different from zero [i.e., $\epsilon_i=0$ if $i\neq 0$ and $\epsilon_0=x$ in Eq. (3.1)], will be scattered (reflected) by the impurity with probability R, where

$$R(x)=x^2/(x^2+4t^2). \quad (4.16)$$

Then if we ignore multiple scattering and treat each site independently, we may calculate the mean free path of an electron at the Fermi energy in our random system. The mean probability of scattering per site is given by

$$\frac{b}{\Lambda_{dc}}=\int dx\,h(x)R(x), \quad (4.17)$$

where $h(x)$ is the probability distribution of the site energies x. For our Gaussian distribution of width St, we find

$$\frac{b}{\Lambda_{dc}}=1-(2\pi)^{1/2}S^{-1}\exp\left(\frac{2}{S^2}\right)\operatorname{erfc}\left(\frac{\sqrt{2}}{S}\right)$$
$$\sim\sum_m(-1)^{m+1}\left(\frac{4}{S^2}\right)^{-m}1\times3\times\cdots\times(2m-1), \quad (4.18)$$

where the expansion is strictly valid only for small S. Retaining only the leading term in the expansion we find

$$\Lambda_{dc}\approx\frac{4b}{S^2}=0.43\,Lb, \quad (4.19)$$

where we have used a relation between the randomness S and the localization length L from Ref. 30. This value of Λ_{dc} is only slightly larger than Λ_{opt} which was computed above. It is also interesting to note that the mean free path is nearly equal to the decay length for probability, which is half that for wave functions.

V. METHOD OF CALCULATION

In addition to these simple models, it is possible to calculate the exact RPA dielectric function for our system. That is we can write integral equations whose solutions will enable us to evaluate the dielectric function from Eq. (3.5). The derivation of these equations follows that of Halperin[35] for the spectral density of various one-dimensional systems and for the conductivity at zero wave vector of a one-dimensional system with a Gaussian white-noise potential.

We write our wave functions in terms of tight-binding states $|n\rangle$,

$$|k\rangle = |\psi(E_j)\rangle = \sum_n a_n(E_j)|n\rangle . \tag{5.1}$$

Choose boundary conditions as follows. Let $a_0(E_j)$ be a real number. Choose a real number Z_L, independent of E, and require

$$a_0(E_j) = Z_L a_1(E_j) . \tag{5.2}$$

Similarly, at the other end of the chain choose a real number Z_R and require

$$a_N(E_j) = Z_R a_{N+1}(E_j) . \tag{5.3}$$

Conditions (3.1), (5.2), and (5.3) can be satisfied simultaneously only at certain energies E_j. These are the eigenvalues of the system. We complete the definition of the eigenfunctions by requiring that they be normalized on a chain N sites in length,

$$\sum_n a_n^2(E_j) = 1 . \tag{5.4}$$

If we relax the condition (5.3), we note that we can construct wave functions $\psi(E)$ at any energy we choose. These wave functions will be normalized on a chain containing N sites, and will coincide with the eigenfunction $|j\rangle$ if and only if $E = E_j$. This can only occur if $a_N(E)/a_{N+1}(E) = Z_R$.

We rewrite Eq. (3.5) as a double integral over energy by introducing δ functions,

$$\langle \epsilon(q,\omega)\rangle = 1 - \lim\left(\frac{8\pi e^2}{q^2 V_c N}\right)\Big\langle \iint dE\, dE' \times \left|\langle\psi(E)|\, e^{i\vec{q}\cdot\vec{r}}\,|\psi(E')\rangle\right|^2 [f(E) - f(E')] \times (E - E' - \hbar\omega + i\hbar\alpha)^{-1} \sum_{jj'} \delta(E - E_j) \times \delta(E' - E_{j'})\Big\rangle \quad . \tag{5.5}$$

We have also introduced $\psi(E)$ defined above, and summed over the spin coordinate s.

By the assumption (3.3) we have

$$\langle\psi(E)|\, e^{i\vec{q}\cdot\vec{r}}\,|\psi(E')\rangle = \sum_n e^{i\vec{q}\cdot\vec{r}_n}\, a_n(E)\, a_n(E') . \tag{5.6}$$

Define a function $Z(n, E)$ by

$$Z(n, E) = a_{n-1}(E)/a_n(E) . \tag{5.7}$$

In terms of this definition the above boundary conditions [Eqs. (5.2) and (5.3)] become

$$Z(1, E) = Z_L, \quad Z(N+1, E) = Z_R . \tag{5.8}$$

The matrix elements in Eq. (5.5) may be rewritten according to Eq. (5.6); the δ functions may be replaced by δ functions in $Z(N+1, E)$, using Eq. (5.8); and the Fermi factors and energy denominator may be removed from the ensemble average. With these changes Eq. (5.5) becomes

$$\langle \epsilon(q,\omega)\rangle = 1 - \lim\left(\frac{8\pi e^2}{q^2 V_c N}\right) \iint dE\, dE' [f(E) - f(E')](E - E' - \hbar\omega + i\hbar\alpha)^{-1} \times \left\langle \left| \sum_n e^{-i\vec{q}\cdot\vec{r}_n} a_n(E) a_n(E') \right|^2 \frac{\partial Z(N+1, E)}{\partial E}\, \delta(Z(N+1, E) - Z_R) \frac{\partial Z(N+1, E')}{\partial E'}\, \delta(Z(N+1, E') - Z_R) \right\rangle . \tag{5.9}$$

All of the information about the Hamiltonian and the randomness is contained within the angular brackets of the above equation. The integral would become straightforward if we could evaluate the quantity in the angular brackets. What follows here is a derivation of an integral for that quantity in terms of auxiliary functions to be defined below for which we shall derive integral equations.

We shall show that the quantity in angular brackets is $NC(q, E, E')$, where C is independent of N, Z_L, and Z_R. Now Eq. (5.9) becomes

$$\langle \epsilon(q,\omega)\rangle = 1 - \lim\left(\frac{8\pi e^2}{q^2 V_c}\right) \iint dE\, dE' [f(E) - f(E'] \times (E - E' - \hbar\omega + i\hbar\alpha)^{-1} C(q, E, E') . \tag{5.10}$$

The integral in Eq. (5.10) may be written in terms of dimensionless energies by scaling all energies to the hopping matrix element t. If this is done, it becomes clear that $\epsilon - 1$ is proportional to e^2/t. Throughout the remainder of this section we assume this scaling has been done.

To evaluate C we define another set of functions and relations among them: Let

$$U(E, n) = \sum_{l=1}^{n-1} \frac{a_l^2(E)}{a_n^2(E)} \tag{5.11}$$

and

$$W(q, E, E', n) = \sum_{l=1}^{n-1} [e^{-i\vec{q}\cdot i\vec{b}} a_l(E)\, a_l(E')] \times [e^{-i\vec{q}\cdot n\vec{b}} a_n(E)\, a_n(E')]^{-1} . \tag{5.12}$$

From these definitions it follows that

$$U(E, n+1) = Z^2(n+1, E)\,[U(E, n) + 1] \tag{5.13}$$

and

$$W(q, E, E', n+1) = e^{i\vec{q}\cdot\vec{b}} Z(n+1, E)\, Z(n+1, E') \times [W(q, E, E', n) + 1] . \tag{5.14}$$

From Schrödinger's equation and Eq. (5.7) we have

$$Z(n+1, E) = [E - \epsilon_n - Z(n, E)]^{-1}, \tag{5.15}$$

so that

$$-\frac{\partial Z(n+1, E)}{\partial E} = Z^2(n+1, E)\left(1 - \frac{\partial Z(n, E)}{\partial E}\right). \tag{5.16}$$

By a comparison of Eqs. (5.16) and (5.13), and taking the boundary conditions at $n = 1$ into account [from which we have $U(E, 1) = \partial Z(1, E)/\partial E = 0$; see Eqs. (5.8) and (5.11)], we observe that

$$U(E, n) = -\frac{\partial Z(n, E)}{\partial E} . \tag{5.17}$$

The quantity in angular brackets in Eq. (5.9) may be rewritten

$$\left\langle \frac{|W(q, E, E', N+1)|^2}{U(E, N+1)\, U(E', N+1)} \frac{\partial Z(N+1, E)}{\partial E} \frac{\partial Z(N+1, E')}{\partial E'} \times \delta(Z(N+1, E) - Z_R)\, \delta(Z(N+1, E') - Z_R) \right\rangle$$

$$= \langle |W(q, E, E', N+1)|^2\, \delta(Z(N+1, E) - Z_R) \times \delta(Z(N+1, E') - Z_R) \rangle . \tag{5.18}$$

We further define the auxiliary functions $P_2(\phi, \phi', n)$, $P_1(\phi, \phi', n)$, and $P_0(\phi, \phi', n)$ by

$$P_0(\phi, \phi', n) = \langle \delta(\tan^{-1} Z(n, E) - \phi) \times \delta(\tan^{-1} Z(n, E') - \phi') \rangle , \tag{5.19}$$

$$P_1(\phi, \phi', n) = \frac{\langle W(q, E, E', n)\, \delta(\tan^{-1} Z(n, E) - \phi)\, \delta(\tan^{-1} Z(n, E') - \phi') \rangle}{(\tan^2\phi + 1)^{1/2} (\tan^2\phi' + 1)^{1/2}} , \tag{5.20}$$

and

$$P_2(\phi, \phi', n) = \langle |W(q, E, E', n)|^2 \times \delta(Z(n, E) - \tan\phi)\, \delta(Z(n, E') - \tan\phi') \rangle . \tag{5.21}$$

We see, by comparison of Eqs. (5.21), (5.18), and (5.17) that the quantity in the large angular brackets in Eq. (5.18) is $P_2(\tan^{-1} Z_R, \tan^{-1} Z_R, N+1)$. Thus we need only to evaluate P_2 in order to compute the dielectric function from Eq. (5.10).

In order to evaluate P_2 we shall derive expressions for $P_j(\phi, \phi', n+1)$ in terms of $P_j(\phi, \phi', n)$ and $P_k(\phi, \phi', m)$, with $k < j$, and $m = n$ or $n+1$.

We begin with the simplest case:

$$P_0(\phi, \phi', n+1) = \langle \delta(\tan^{-1}[E - \epsilon_n - Z(n, E)]^{-1} - \phi) \times \delta(\tan^{-1}[E' - \epsilon_n - Z(n, E')]^{-1} - \phi') \rangle . \tag{5.22}$$

As we have seen above, $Z(n, E)$ depends only on Z_L and ϵ_l for $l < n$, and not on ϵ_n. This expectation value may then be written

$$P_0(\phi, \phi', n+1) = \int d\epsilon_n\, h(\epsilon_n) \times \langle \delta(\tan^{-1}[E - \epsilon_n - Z(n, E)]^{-1} - \phi) \times \delta(\tan^{-1}[E' - \epsilon_n - Z(n, E')]^{-1} - \phi') \rangle , \tag{5.23}$$

where $h(\epsilon_n)$ is the probability density function for the random variable ϵ_n, a Gaussian of width S.

The arguments of the δ functions may be transformed into the form $\delta(\tan^{-1} Z(n, E) - \tan^{-1}(E - \epsilon_n - 1/\tan\phi))$ by multiplying the δ function by $\partial \tan^{-1}(E - \epsilon_n - 1/\tan\phi)/\partial\phi$. In this way we obtain

$$P_0(\phi, \phi', n+1) = (\sin\phi \sin\phi')^{-2} \times \int \frac{d\epsilon_n\, h(\epsilon_n) \langle \delta(\tan^{-1} Z(n, E) - \tan^{-1}(E - \epsilon_n - 1/\tan\phi))\, \delta(\tan^{-1} Z(n, E') - \tan^{-1}(E' - \epsilon_n - 1/\tan\phi')) \rangle}{[1 + (E - \epsilon_n - 1/\tan\phi)^2][1 + (E' - \epsilon_n - 1/\tan\phi')^2]} . \tag{5.24}$$

The quantity in angular brackets is clearly $P_0(\tan^{-1}(E - \epsilon_n - 1/\tan\phi), \tan^{-1}(E' - \epsilon_n - 1/\tan\phi'), n)$, so we find

$$P_0(\phi, \phi', n+1) = (\sin\phi \sin\phi')^{-2} \int \frac{d\epsilon_n h(\epsilon_n)}{1+(E-\epsilon_n - 1/\tan\phi)^2}$$

$$\times \frac{P_0(\tan^{-1}(E-\epsilon_n-1/\tan\phi),\ \tan^{-1}(E'-\epsilon_n-1/\tan\phi'), n)}{1+(E'-\epsilon_n-1/\tan\phi')^2} \ . \tag{5.25}$$

By a similar argument, starting from Eq. (5.20) and making use of Eq. (5.14), we have

$$P_1(\phi, \phi', n+1) = e^{i\vec{q}\cdot\vec{b}} (\sin\phi \sin\phi')^{-1} \int \frac{d\epsilon_n h(\epsilon_n)}{[1+(E-\epsilon_n-1/\tan\phi)^2]^{1/2}}$$

$$\times \frac{P_1(\tan^{-1}(E-\epsilon_n-1/\tan\phi),\ \tan^{-1}(E'-\epsilon_n-1/\tan\phi'), n)}{[1+(E'-\epsilon_n-1/\tan\phi')^2]^{1/2}} + e^{i\vec{q}\cdot\vec{b}} \sin\phi \sin\phi' P_0(\phi, \phi', n+1) \ . \tag{5.26}$$

Similarly, we may show that

$$P_2(\phi, \phi', n+1) = \int d\phi_1 d\phi_1' K(\phi, \phi'; \phi_1, \phi_1') [P_2(\phi_1, \phi_1', n) + 2\cos\phi_1 \cos\phi_1' \mathrm{Re} P_1(\phi_1, \phi_1', n)$$

$$+ \cos^2\phi_1 \cos^2\phi_1' P_0(\phi_1, \phi_1', n)], \tag{5.27}$$

where

$$K(\phi, \phi'; \phi_1, \phi_1') = \int d\epsilon_n h(\epsilon_n) \delta(\phi_1 - \tan^{-1}(E-\epsilon_n-1/\tan\phi)) \delta(\phi_1' - \tan^{-1}(E'-\epsilon_n-1/\tan\phi')) \ . \tag{5.28}$$

A particularly interesting and useful property of these functions P_j is their well-defined behavior as n becomes large,

$$P_0(\phi, \phi', n) \to p_0(\phi, \phi'),$$
$$P_1(\phi, \phi', n) \to p_1(\phi, \phi'), \tag{5.29}$$

and

$$P_2(\phi, \phi', n) \to nC + f(\phi, \phi', n),$$

where p_0, p_1, and C are independent of n, C is independent of ϕ and ϕ', and f is of order n^0 or smaller, so that for large n, $P_2/n \to C$. The proofs of these statements are given in the Appendix.

In the Appendix, we also show that C may be written as an integral of the functions p_0 and p_1,

$$C = \int d\phi\, d\phi'\, p_0(\tan^{-1}(1/\tan\phi), \tan^{-1}(1/\tan\phi'))$$
$$\times \{2\cos\phi \cos\phi' \mathrm{Re}[p_1(\phi, \phi')] + \cos^2\phi \cos^2\phi'$$
$$\times p_0(\phi, \phi')\} \ . \tag{5.30}$$

We observe finally that the C in Eq. (5.30) is the same as the C in Eq. (5.10). Thus the quantity C may be calculated by solving two integral equations [Eqs. (5.25) and (5.26)] and doing one integral [Eqs. (5.30)] for each pair of energies. From this point an integral over the two energies E and E' [Eq. (5.10)] is required to compute the dielectric function.

VI. NUMERICAL PROCEDURES

Equations (5.25) and (5.26) have no analytic solutions, so it was necessary to solve them numerically. This entailed discretizing the space of the ϕ, ϕ' coordinates, which proved to be the most difficult phase of the project. We had two tests of the quality of our choice of discretization. First, Eq. (5.25) is a homogeneous equation, of the form $\int K p_0 = \lambda p_0$, with $\lambda = 1$. We calculated p_0 by starting with an initial guess $P_0^{(0)}$, computing $P_0^{(1)\prime} = M P_0^{(0)}$, where M is a discretization of the kernel, and normalizing $P_0^{(1)\prime}$ to form $P_0^{(1)}$. The $P_0^{(i)}$ were formed in this way until P_0 at each grid point changed by less than 0.002 of its value in one iteration step. [We tried several other methods—successive over-relaxation (SOR),[36,37] Aitken's δ^2 process,[38] and Wynn's ϵ algorithm,[39] but none of these led to any reduction in the computer time required to produce convergence.] If p_0 is the converged result of such an algorithm suitably normalized the largest eigenvalue of the matrix is the number by which $p_0' = M p_0$ must be divided in order to normalize it. One test of the adequacy of a particular grid is the closeness of this eigenvalue to one.

The second test is the value of C [from Eq. (5.30)] at zero wave vector. For small wave vector C reduces to

$$C(q, E, E') = q^2 \Big\langle \sum_{kk'} |\langle k| x |k'\rangle|^2 \delta(E-E_k) \times \delta(E'-E_{k'}) \Big\rangle \Big/ N \ . \tag{6.1}$$

For a random one-dimensional system all states are localized,[28] so the matrix element in Eq. (6.1) is finite for any k and k'. Hence $C(q=0) \to 0$

as q^2. By computing the value of C at zero wave vector for a particular discretization, and comparing that value with typical values for nonzero wave vectors, we were able to produce another test of the accuracy of that particular discretization.

As our first method of discretization, we approximated the function by its values on a square grid of points, typically choosing 12-20 points on a side. It soon became clear that the functions involved were not sufficiently smooth for this sort of approximation, unless we were to use impractically large numbers of points.

We then tried a scheme in which the functions were evaluated at points which were intersections of the "natural lines" of the problem. Equations (5.25) and (5.26) are line integrals in a two-dimensional space. Further, each such line of integration (type A) generates values of the functions for an entire subset of ϕ, ϕ' points, which form another line (type B) in the space. If a subset of lines is chosen from the infinite set of possible lines of integration, a subset of lines of type B is also singled out. The intersections of the lines of type A with the lines of type B were taken as the points of the grid. This scheme was also unsatisfactory. We found no practical way to do the two-dimensional integral in Eq. (5.30), or even to calculate $p_0(\tan^{-1}(1/\tan\phi), \tan^{-1}(1/\tan\phi'))$, which is one factor in that integral. Besides this, we were unable to obtain as good solutions to Eq. (5.27) with this method as we could with the method described below. That is, this method gave an eigenvalue of 0.85 for about the same number of points that our final method gave an eigenvalue of 0.95, at $E=1.75$, $E'=1.25$, $S=2.00$. Another difficulty with this method arose in choosing the lines. Each grid was a single point in an (approximately) 20-dimensional vector space; choosing an optimum set of lines by hand or by machine was a nontrivial task.

We finally decided on a square mesh of points with variable density. That is the square of side π in ϕ, ϕ' space was subdivided into smaller squares, and the point density in each subsquare could be 1, 4, 16, or 64 times the minimum density. (Or alternatively, the distance between adjacent points of each smaller square could be 1, 2, 4, or 8 times the minimum distance.) The minimum distance between points was usually $\frac{1}{64}\pi$, but sometimes $\frac{1}{96}\pi$, or even $\frac{1}{128}\pi$ was necessary. We typically chose grids of 400-500 points (Fig. 1), but occasionally were forced to use as many as 1200.

At first we chose the positions of the fine density grids by hand, but as we built up experience working with the problem we were able to devise a semiautomatic program for grid placement. This program interpolated p_0 in energy space to a trial grid at a new energy point, and modified the grid to reduce the projected error. (The projected error is a quantity we defined to approximate the anticipated contribution of each region to the total error in the function p_0. It is the product of the maximum value of the third difference in the square, the mean value of the function p_0 in the square, and the number of points whose lines of integration—lines of type A, described above—pass through the square.) p_0 was then interpolated to this new grid from its known values at other points in the energy plane as before, and, if necessary, modified again. This process was repeated until convergence was obtained. Then the integral equation was solved on the chosen grid with the interpolated function as the initial trial value of p_0.

To solve Eqs. (5.25) and (5.26) it was then necessary to reduce the integral kernal to matrix form. Each row of the matrix represents a single line integral. These line integrals do not, in general, pass through any of the grid points except the corners $(-\frac{1}{2}\pi, -\frac{1}{2}\pi)$ and $(\frac{1}{2}\pi, \frac{1}{2}\pi)$. Wherever a line of the grid crossed a line of integration we interpolated to the intersection from the three nearest grid points. We then divided the line of integration into segments, each containing three interpolated points, and approximated the unknown function by a quadratic polynomial in each segment. We next did the integrals of kernel times polynomial in each segment using the six

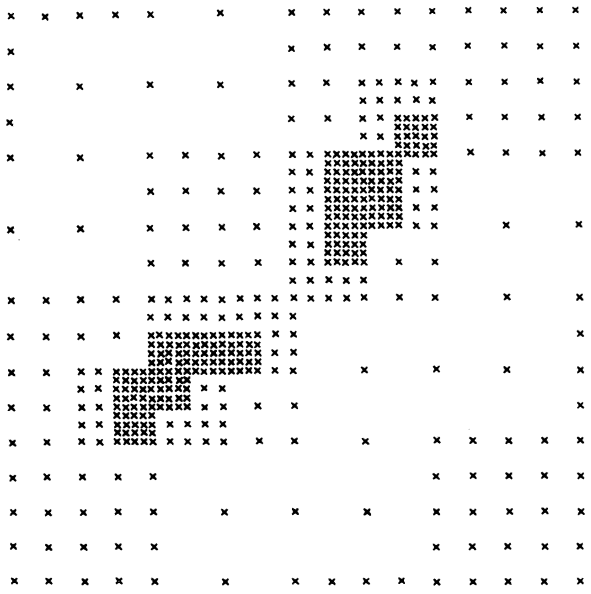

FIG. 1. Grid of 464 points, on which p_0, p_1, and C were computed at $E=0.50$, $E'=0.0$. Grids we used for most energy pairs were similar to this one.

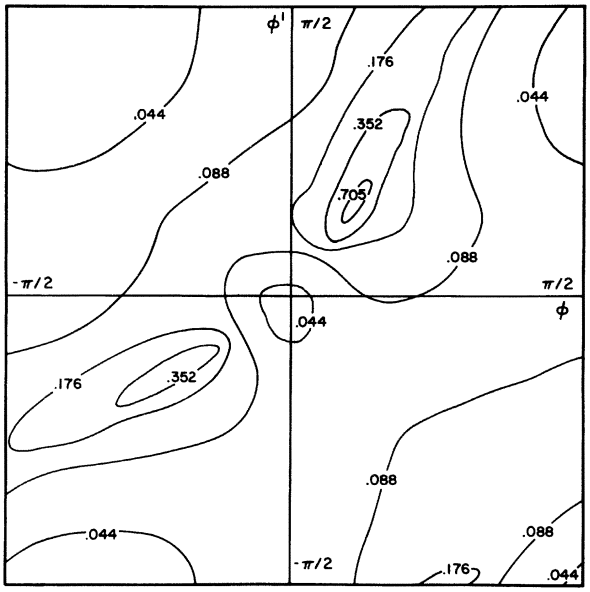

FIG. 2. Contour plot of $p_0(\phi, \phi')$ for $E = 0.50$, $E' = 0.0$, and $S = 1.0$, computed on the grid of Fig. 1.

point Gauss-Lagrange integration formula. In this way we were able to produce matrices to represent the kernels for both integral equations. In fact the kernels for the two Eqs. (5.25) and (5.26) are so similar that we were able to produce both matrices simultaneously for a given randomness value and energy pair.

Having set up the matrix, we solved for p_0 by straightforward iteration, as described above. Of the eigenvalues we computed for randomness $S = 1$, 59% were within 1% of the predicted value of 1.0, and 87% were within 0.02. The remainder were far out in the tails of the energy band, where the contributions to the dielectric function were small. For randomness $S = 1.5$, 42% of the eigenvalues were in the interval 1.00 ± 0.01, and 84% were within 0.02 of 1. Of those with more than 2% error, three were out near the edges of the band, but two were near $E - E' = 0$; this suggests that the error in the low-frequency dielectric function may be greater in this case than for $S = 1$. A sample p_0 is shown in Fig. 2.

The quantity p_1 was calculated from Eq. (5.26) in a similar way, except that in this case we had no normalization criterion to use, so p_1 was not renormalized at each step. We also found that SOR with relaxation parameter $\omega = 1.1$[36,37] provided faster convergence than simple iteration.

Before doing the final integration, we calculated p_0 and p_1 at $(\tan^{-1}(1/\tan\phi), \tan^{-1}(1/\tan\phi'))$, when these points were not on the original grid. We calculated these new values of p_0 and p_1 by inserting the known values on the right-hand side of the integral equation, and doing a single integration like that involved in setting up the matrix. The integral in Eq. (5.30) was done one subsquare at a time, using Simpson's rule in both directions.

At randomness 1, the values we calculated for $C(q = 0)$ were typically 10^{-3} to 10^{-4}, and very near $E = E'$ they rose to 10^{-2}. For $q \neq 0$, the values of C were typically in the range of 10^{-1}–10^{-2} except at very large energies, where they tailed off. From this we argue that the significant values of C have errors of the order (1–3)% in most cases.

The values of $C(q = 0)$ at randomness 1.5 were typically in the range 10^{-3}–10^{-4}, but for very small $E - E'$ they rose rapidly to become greater than 10^{-2}. We were unable to correct this behavior with any grid of practical size. To compensate for these errors, we subtracted the value of $C(q = 0)$ from that of $C(q = 0.1)$ whenever it appeared that the calculated value of $C(q = 0.1)$ was appreciably in error, as shown by the error in $C(q = 0)$.

It was only necessary to evaluate C over one-fourth of the area in the energy band squared. One factor of $\frac{1}{2}$ came from the symmetry of C in its two energy indices: $C(E, E') = C(E', E)$. The other factor of $\frac{1}{2}$ came from the symmetry about $E = 0$ of both the unperturbed band and the chosen form of disorder. From this we obtained $C(E, E') = C(-E, -E')$.

We evaluated the integral in Eq. (5.10) by first integrating along lines of constant $\hbar\omega_0 = E - E'$, in this way computing $\epsilon_2(q, \omega_0)$. When these integrals were done, we did the integral over $E - E'$, effectively calculating ϵ_1 from ϵ_2 by Kramers-Kronig analysis. Both of these integrals were done treating the numerator as a cubic polynomial in the variable of integration and treating the denominator analytically. We also did the integrals approximating the numerators as quadratic instead of cubic, with no significant change in the result.

We evaluated the dielectric function at $T = 0$ only. It was not necessary, therefore, to evaluate C at energy pairs E, E' for which E and E' were on the same side of the Fermi level, since $f(E) - f(E') = 0$ for these pairs.

Because of the q^2 in the denominator of Eq. (5.10), it is impossible to use this form directly to compute $\epsilon(q = 0)$. We took advantage of Eq. (6.1) to remove this apparent singularity. To do the calculation we defined a quantity C^*,

$$C^*(E, E') = \left\langle \sum_{kk'} |\langle k|[H, r]|k'\rangle|^2 \times \delta(E - E_k)\,\delta(E' - E_{k'}) \right\rangle \Big/ Nb^2 . \quad (6.2)$$

We were able to define P_1^*, p_1^*, and P_2^* by analogy P_1, p_1, and P_2, and by arguments similar to those given in Sec. V, we established that

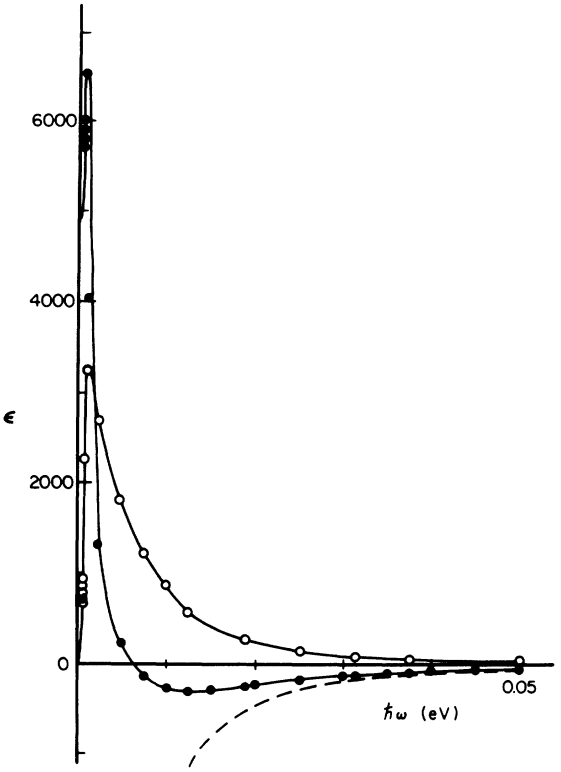

FIG. 3. Longitudinal dielectric function vs frequency for randomness $S=1.0$ and wave vector $q=0.0$. Other parameters are $T=0$; transfer matrix element $t=0.025$ eV; volume of a unit cell $V_c=470.7$ Å^3; lattice constant along the chains $b=3.87$ Å; half-filled band. Filled circles, ϵ_1; open circles, ϵ_2; dashed line, ϵ_1^c (real part of the crystalline dielectric function).

$$p_1^*(\phi,\phi') = (\sin\phi\,\sin\phi')^{-1}\int \frac{d\epsilon\, h(\epsilon)}{[1+(E-\epsilon-1/\tan\phi^2]^{1/2}} \times \frac{p_1^*(\tan^{-1}(E-\epsilon-1/\tan\phi),\, \tan^{-1}(E'-\epsilon-1/\tan\phi'))}{[1+(E'-\epsilon-1/\tan\phi')^2]^{1/2}} + [\sin\phi\,\sin\phi'(E-E')+\sin(\phi-\phi')]p_0(\phi,\phi') \tag{6.3}$$

and

$$C^*(E,E') = \int d\phi\, d\phi'\, p_0(\tan^{-1}(1/\tan\phi),\, \tan^{-1}(1/\tan\phi')) \times [2\sin(\phi-\phi')p_1^*(\phi,\phi') + \sin^2(\phi-\phi') \times p_0(\phi,\phi')]\,. \tag{6.4}$$

From this and Eq. (5.10) we have

$$\epsilon(q=0,\omega) = 1 - \lim_{\alpha\to 0^+}\frac{8\pi e^2 b^2}{V_c} \times \iint \frac{dE\,dE'\,C^*(E,E')}{(E-E')^2\,(E-E'-\hbar\omega+i\hbar\alpha)}\,. \tag{6.5}$$

We evaluated the quantities C^* and $\epsilon(q=0)$ by methods analogous to those described above for finite wave vectors.

The $(E-E')^2$ in the denominator of Eq. (6.5) implies that C^* should go to zero quadratically in $E-E'$ if ϵ is to be finite. This will occur in an exact solution since

$$C^*(E,E') = \lim_{q\to 0} C(q,E,E')\,(E-E')^2/(qb)^2\,,$$

as may be seen by comparison of Eqs. (6.2) and (6.1), and, as we have argued above, $C(q,E,E')/q^2$ tends to a finite value as $q\to 0$. Errors in the calculated C^* obscured this quadratic behavior. We shall defer until Sec. VII for a description of our treatment of C^* for small $E-E'$.

VII. RESULTS AND DISCUSSION

We have computed the longitudinal dielectric function for a system in which the randomness $S=1$, for wave vectors 0.0, 0.125, 0.2, 0.5, 0.9, and 1.0, in units of π/b, where b is the lattice constant along the chain, and for a system with $S=1.5$, for wave vectors 0.0, 0.1, and 0.2. The other parameters were chosen to match the experimental values or best guesses for NMP-TCNQ: nearest-neighbor hopping matrix element $t=0.025$ eV,[6] lattice constant $b=3.8682$ Å, and volume of a unit cell $V_c=470.7$ Å^3.[12] These parameters merely fix the energy and magnitude scales of the dielectric function, and do not affect its shape. We find that

$$\epsilon = 1 + G(qb,\, \hbar\omega/t,\, kT/t,\, S)\,(b^2/tV_c)\,, \tag{7.1}$$

where G is a function independent of the parameters b, t, and V_c.

The results are shown in Figs. 3–11. In these graphs we show the real and imaginary parts of the dielectric function, ϵ_1 and ϵ_2, as functions of frequency for the given wave vector. We also show for comparison ϵ_1^c and ϵ_2^c, the real and imaginary parts of the dielectric function for a crystalline tight-binding band with the same cell dimensions and hopping element. The expressions used for ϵ_1^c and ϵ_2^c are identical to those derived by Williams and Bloch[40] [their Eqs. (18) with $\theta=0$ and $\epsilon_\infty=1$], except that our ϵ_2^c is twice as large as theirs, as is necessary to satisfy Kramers-Kronig relations.

In what follows we discuss ϵ_2 first, then ϵ_1, then the plasma frequency, and finally the ac conductivity.

A. Imaginary part

At all wave vectors the curve of ϵ_2 looks like a broadened form of that for ϵ_2^c. A similar broadening has been observed in the optical absorption spectra of amorphous and crystalline forms of

certain semiconductors.[41] Because the peak position is shifted very little between the crystalline and random curves, the wave functions in the random system are likely similar to those in the crystalline system, but exponentially damped:

$$\psi_k \approx e^{ikx-|x-x_k|/Lb}.$$

In Sec. IV A we observed that states of this form lead to an ϵ_2 which is peaked at $\hbar\omega = 2qbt$ but with width $4t/L$. Figures 4, 5, 10, and 11, for which the wave vectors are sufficiently small that the peak in ϵ_2 is at low frequency, demonstrate the behavior clearly. The peak position in each of these curves is where the crystalline peak occurs (at $4t\sin\frac{1}{2}qb \approx 2qbt$), and the broadening in Figs. 4 and 5 is about 0.01 eV, and in Figs. 10 and 11 about 0.02 eV; in each case this is $4t/L$. At larger wave vectors (Figs. 6–8) the derivation in Sec. IV is not strictly applicable, but the observed broadening at the high-frequency end of ϵ_2 is also about 0.01 eV.

We note in passing that $\epsilon_2^c = 0$ for $|\hbar\omega| < |2\sin qb|$ in one dimension. Energy conservation requires a minimum energy change of $|2t\sin qb|$

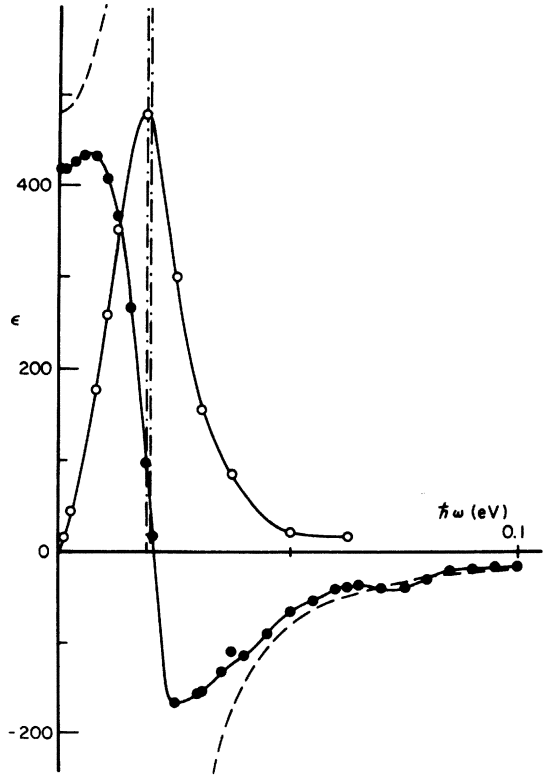

FIG. 4. Longitudinal dielectric function vs frequency for $S = 1.0$ and $q = 0.125\ \pi/b$. The imaginary part of the crystalline dielectric function, ϵ_2^c, is greater than 1.96×10^4 between the dot-dashed lines. Other parameters are the same as in Fig. 3.

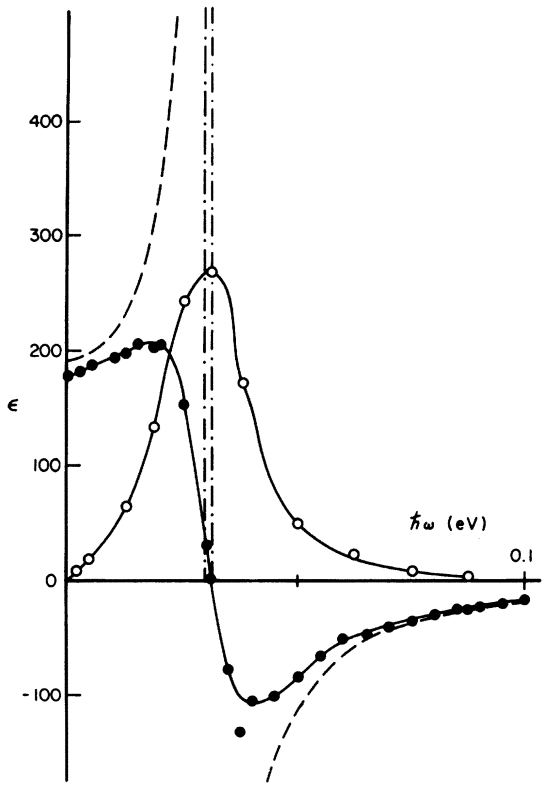

FIG. 5. Longitudinal dielectric function vs frequency for $S = 1.0$ and $q = 0.20\ \pi/b$. ϵ_2^c is greater than 3.05×10^3 between the dot-dashed lines. Other parameters are the same as in Fig. 3.

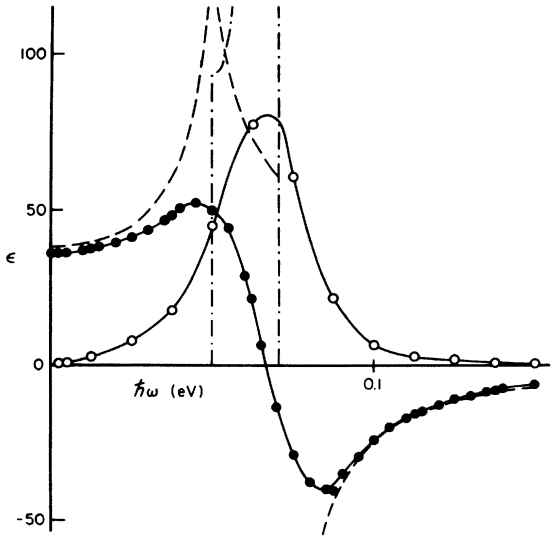

FIG. 6. Longitudinal dielectric function vs frequency for $S = 1.0$ and $q = 0.50\ \pi/b$. The dot-dashed line shows ϵ_2^c. Other parameters are the same as in Fig. 3.

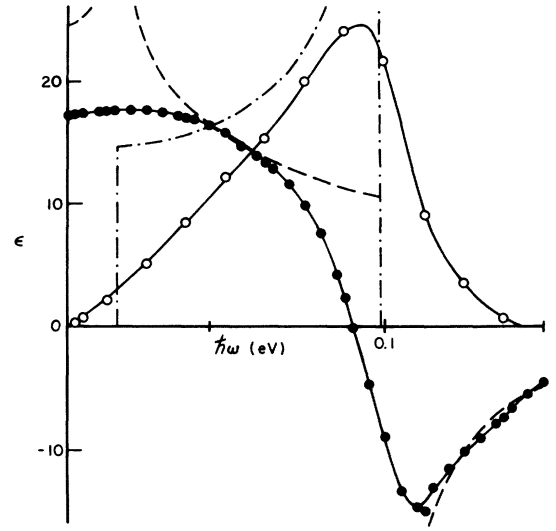

FIG. 7. Longitudinal dielectric function vs frequency for $S=1.0$ and $q=0.9\,\pi/b$. Other parameters are the same as in Fig. 3.

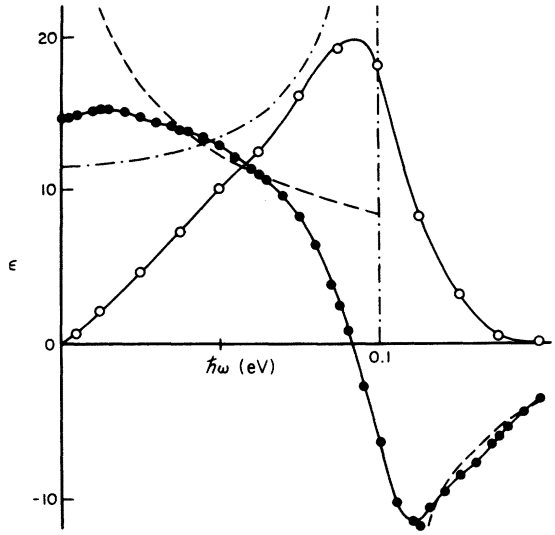

FIG. 8. Longitudinal dielectric function vs frequency for $S=1.0$ and $q=\pi/b$. Other parameters are the same as in Fig. 3.

for a transition under a perturbing potential of wave vector q. This minimum energy change is required because the one-dimensional Fermi surface consists of two points. It is not possible to create a transition between states the differences between whose k vectors lies nearly along the Fermi surface as one can in two and three dimensions. Energy conservation also requires $\epsilon_2^c = 0$ for $|\hbar\omega| > |4t \sin\frac{1}{2} qb|$.

B. Real part

As might be expected from the discussion of ϵ_2 above, the real part of the dielectric function resembles that in the crystalline case, but with the singularities smeared out. In general, as the frequency increases, ϵ_1 rises from its $\omega = 0$ value to a maximum, drops sharply to its largest negative value, then increases slowly to one. The positive

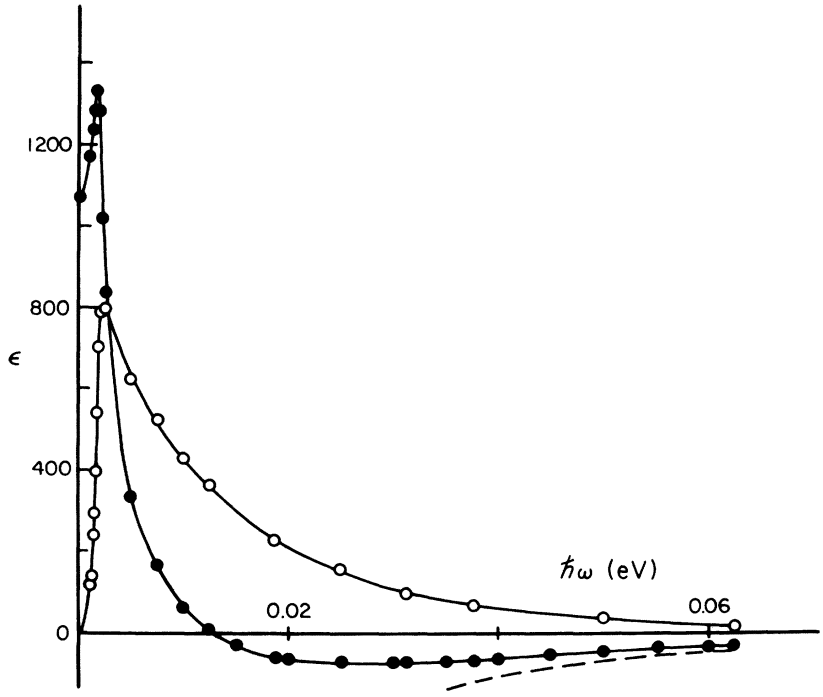

FIG. 9. Longitudinal dielectric function vs frequency for $S=1.5$ and $q=0.0$. Other parameters are the same as in Fig. 3.

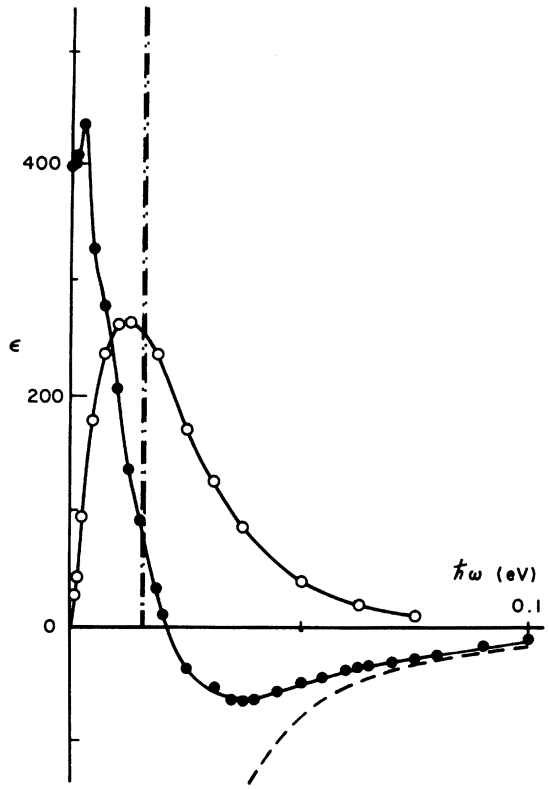

FIG. 10. Longitudinal dielectric function vs frequency for $S=1.5$ and $q=0.10\ \pi/b$. ϵ_2^c is greater than 4.76×10^4 between the dot-dashed lines. Other parameters are the same as in Fig. 3.

and negative peaks are shifted by about $4t/L$ from the position of the crystalline singularities; the magnitude of the shift is the same as the amount of broadening observed in ϵ_2.

The small secondary minimum in ϵ_1 ($0.125\ \pi/b$, ω) for $S=1$ near $\hbar\omega=0.70$ eV is probably an artifact of the calculation, a result of our inability to obtain accurate values of C for $C<10^{-4}$. We ran the calculation once more adding small positive values of C along $E-E'=0.075$ eV (where we have no computed values), and once with the values of C along $E-E'=0.060$ eV reduced by a factor of 2. (Either of these changes provides a smoother decrease of ϵ_2 to zero.) In both cases the extra minimum in ϵ_1 disappeared.

One striking feature of these results is that ϵ_1 is finite at zero frequency and wave vector. Because of the localization of all the states by the randomness, the dc conductivity vanishes at $T=0$, as discussed further below, leading to a finite $\epsilon_1(0,0)$. This remains true at finite temperature in our model because we have omitted phonon-assisted hopping as a mechanism for producing dc conductivity. When the effects of phonons are included, the Thomas-Fermi form of $\epsilon(q,\omega)$ holds for small q and ω smaller than the hopping rates.

For finite but small wave vector ($qb\leq 0.2\pi$) we made the analytic approximation

$$\epsilon_1^A(q,0)=1+\frac{u\kappa^2}{q^2+r/L^2b^2}\ , \tag{7.2}$$

where u and r are parameters chosen to fit the data. Figure 12 is a plot of $\kappa^2L^2b^2/(\epsilon-1)$ vs $(qLb)^2$. The best fit to a straight line through the four points with $0.1\pi\leq qb\leq 0.2\pi$ (which are free of the uncertainty in C^* near $E-E'=0$) gives $u=0.993$ and $r=1.560$, which are very close to $u=1$ and $r=\frac{1}{2}\pi$. The agreement with the extrapolation [Eq. (4.12)] is surprisingly good. The calculated values for the dielectric constant at $q=0$ are also in approximate agreement; for them $r/u=1.3$.

For wave vectors larger than $0.2\pi/b$, the dielectric constant rises above the Thomas-Fermi value of $1+\kappa^2/q^2$. (It is about twice as large as $1+\kappa^2b^2/\pi^2$ at $q=\pi/b$; see Fig. 13.) This excess is all that remains of the logarithmic singularity in ϵ_1 at $q=2k_F$ which gives rise to the Peierls distortion[42] in the perfect crystal. The condition for the occurrence of the Peierls distortion[43] is

$$\hbar\omega(2k_F)\leq g^2(2k_F)(2k_F)^2[\epsilon_1(2k_F,0)-1]V_c/8\pi e^2\ , \tag{7.3}$$

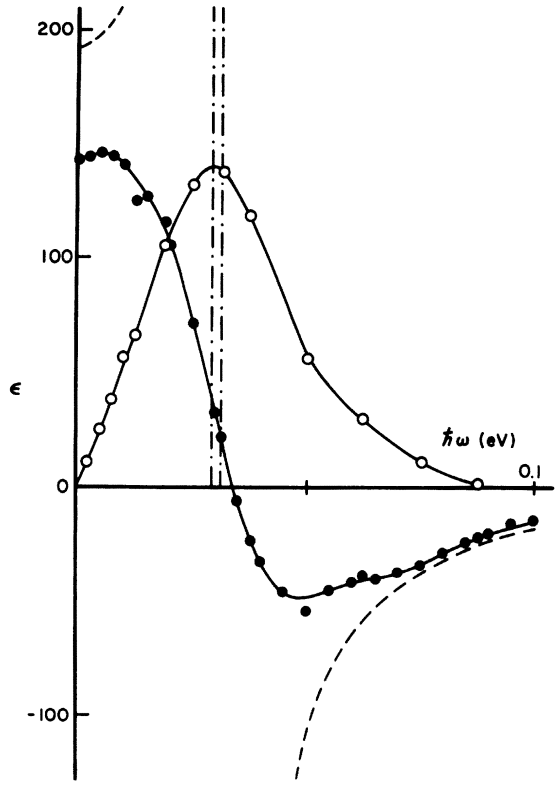

FIG. 11. Londitudinal dielectric function vs frequency for $S=1.5$ and $q=0.20\ \pi/b$. ϵ_2^c is greater than 3.05×10^3 between the dot-dashed lines. Other parameters are the same as in Fig. 3.

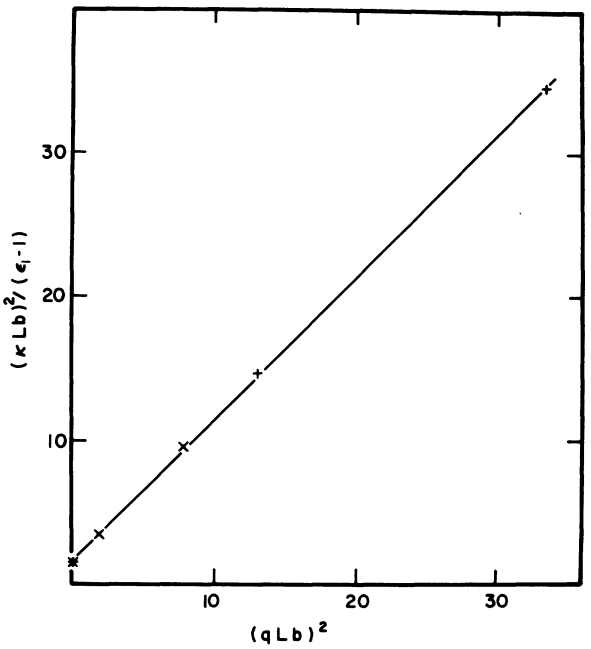

FIG. 12. $(\kappa Lb)^2/[\epsilon_1(q,0)-1]$ vs $(qLb)^2$, where κ is the inverse Thomas-Fermi screening length and L is the exponential decay length of states at the Fermi level. All points for both randomness values with $q \leq 0.2\ \pi/b$ are included. +, $S=1.0$; ×, $S=1.5$.

where $\hbar\omega(q)$ is the energy of a LA phonon at wavevector q, in the absence of electron-phonon coupling and g is the electron-phonon coupling parameter as defined in Ref. 43. We conclude that the electron-phonon coupling constant $\lambda = g^2(2k_F)/4t\hbar\omega$ must be greater than 0.845 for a Peierls distortion to occur at $T=0$ for $S=1$. The energies of acoustic phonons in NMP-TCNQ are of the order of 0.01 eV or less (based on data in Ref. 26), so that an electron-phonon coupling parameter of 0.03 eV would be necessary to produce a Peierls distortion if $S=1$ in NMP-TCNQ. Preliminary analysis of susceptibility data[44] has indicated that S may be as large as three. A Peierls distortion has not been observed in NMP-TCNQ.[13,14] This observation is compatible with our results and any reasonable values of the randomness and electron-phonon coupling. Sen and Varma[45] have calculated the Peierls transition temperature in the coherent potential approximation for some binary alloys; our results support their conclusion that a large electron-phonon coupling is required to maintain a Peierls distortion in the presence of a randomness localizing the electronic states to ten sites.

If our estimate of the transfer matrix element of NMP-TCNQ is correct, Eq. (4.10) with the observed microwave dielectric constant of 350 implies a localization length of 2.75 sites, in good agreement with an estimate of three sites made by Bloch[46] on other grounds. This localization length would be provided by a randomness of S of 1.9. With an analytic form for $\epsilon(L)$ valid at all wave vectors, analogous to Eq. (4.12) for small wave vectors, and using Eq. (3.2) we could produce a set of equations $S=S(\epsilon)$ and $\epsilon=\epsilon(S)$. A solution of those equations could then be compared with the experimental value to determine the extent to which the random ordering of the NMP dipoles influences the dielectric function and localization of the states.

The observed microwave dielectric functions in NMP-TCNQ and the other one-dimensional conductors increase with temperature. We understand the increase in terms of the turning on of phonon-assisted hopping. At very low temperatures, even microwave frequencies are much larger than the jump frequencies associated with hopping. The electrons are effectively localized as a result, and the dielectric function is of the form $\epsilon(q,\omega) = 1 + \kappa^2/[q^2 + \frac{1}{2}\pi/(Lb)^2]$ [Eq. (4.12)]. At

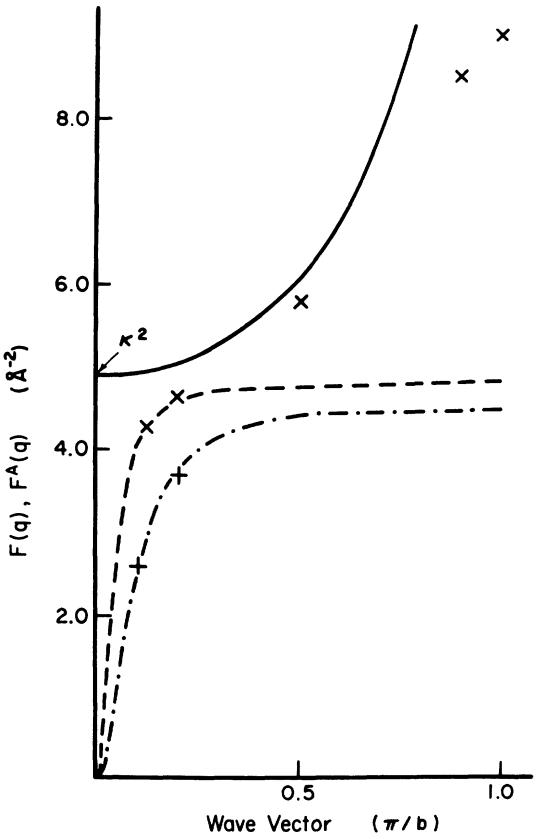

FIG. 13. $F(q) = q^2[\epsilon_1(q,0)-1]$ vs q, and $F^A(q) = q^2 \times [\epsilon_1^A(q,0)-1]$ vs q, where ϵ_1^A is defined by Eq. (7.2). Solid line, $F(q)$ for the crystalline case; ×, $F(q)$ for $S=1.0$; +, $F(q)$ for $S=1.5$; dashed line, $F^A(q)$ for $S=1.0$; dot-dashed line, $F^A(q)$ for $S=1.5$. Note the increase in $F(q)$ above κ^2 at large wave vector.

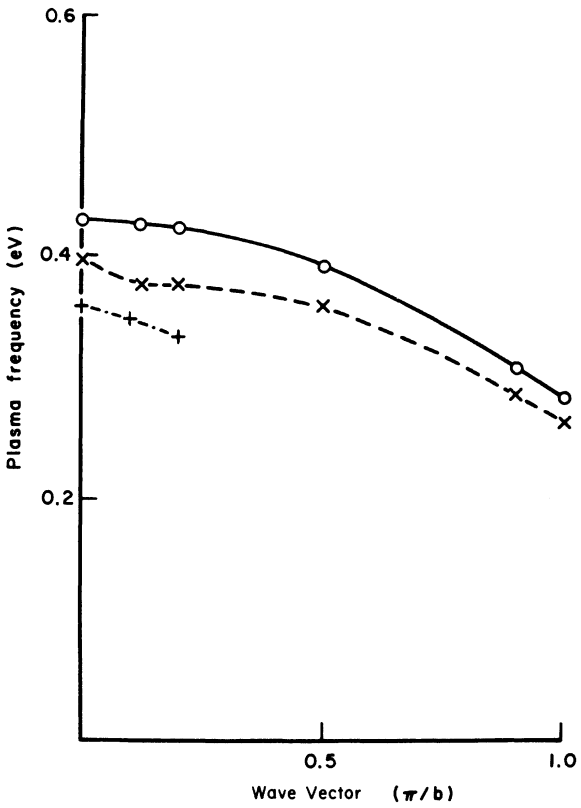

FIG. 14. Plasma frequency vs wave vector. Solid line, crystalline; dashed line, $S=1.0$; dot-dashed line, $S=1.5$.

high temperatures the jump frequencies are much larger. The electrons are no longer bound to their localized states and the dielectric function becomes that of a conductor, $\epsilon = 1 + \kappa^2/q^2$. What is observed is the "turning on" of the hopping, the transition from insulating to conducting behavior, which leads to the increase in ϵ_1.

C. Plasma frequency

Figure 14 is a plot of plasma frequency vs wave vector. At large wave vectors the plasma frequency was determined by finding the higher frequency at which ϵ_1 passed through zero. For small wave vectors, we calculated the plasma frequency from Kramers-Kronig relations

$$\epsilon_1(q,\pi) = 1 + \frac{2}{\pi}\int_0^\infty \omega' \epsilon_2(q,\omega')\,(\omega'^2 - \omega^2)^{-1}\,d\omega' . \tag{7.4}$$

If $\epsilon_2(q,\omega') \approx 0$ for $\omega' > \omega'_{\max}$, and $\omega \gg \omega'_{\max}$, Eq. (7.4) becomes

$$\epsilon_1(q,\omega) = 1 - \omega_p^2(q)/\omega^2, \tag{7.5}$$

where

$$\omega_p^2(q) = \frac{2}{\pi}\int_0^{\omega'_{\max}} \omega' \epsilon_2(q,\omega')\,d\omega' . \tag{7.6}$$

For $q \leq 0.20\,\pi/b$, $\omega_p \gg \omega'_{\max}$, and ω_p was calculated from this expression. As the randomness increases, the plasma frequency decreases. To understand this, we examine Eq. (7.6), and approximate $\omega_p^2 \approx (2/\pi)\bar{\omega}\,\bar{\epsilon}_2 \Delta\omega$, where $\Delta\omega$ is the width of the energy region where ϵ_2 is appreciably different from zero; $\bar{\omega}$ is a mean energy in that region, and $\bar{\epsilon}_2$ is a mean value of ϵ_2 in that region. By inspection of Figs. 3–11 we observe that $\bar{\omega}$ increases by a small amount with increasing randomness and $\Delta\omega$ increases by a large amount, owing to the broadening effect of the randomness as described in Sec. VII A. The mean value of ϵ_2, however, has decreased by a very large factor from the crystalline case (note that ϵ_2^c has a square-root singularity at $\hbar\omega = 4t\sin\frac{1}{2}qb$). We attribute this reduction in ϵ_2 to the localization of the wave functions. Not only will the matrix element be smaller in the random case because the states are not spread out as far, but many pairs of wave functions will not overlap at all, and contribute nothing to the total. The reduction this effect produces in $\bar{\epsilon}_2$ is more than enough to offset the increase observed in $\Delta\omega$ and $\bar{\omega}$.

D. Conductivity

We calculated the frequency and wave-vector dependent electrical conductivity from ϵ_2: $\sigma(q,\omega) = \omega\epsilon_2(q,\omega)/4\pi$. The results are shown in Figs. 15 and 16. In each case the conductivity increases quadratically from zero frequency, reaches a maximum, and decreases again to zero. The widths of the curves, like those for ϵ_2, are inversely proportional to the localization lengths of the states at the Fermi level. The quadratic dependence of the conductivity on frequency for small frequency is clearly observed for finite wave vectors. We were, however, unable to obtain accurate values of C^* for small $E - E'$, and could not therefore calculate σ for small ω directly. We expect a quadratic dependence on frequency in the $q = 0$ case as well (see Sec. IV C or Mott and Davis[34]).

Because of the great success of our analogous formula for $\epsilon_1(q,0)$ we used Eq. (4.14) to determine C^* and ϵ_2 for the small ω region where we had no reliable data before, and used that data, joined smoothly to our C^* values for larger ω, to calculate $\epsilon_1(0,\omega)$. The values we have computed for ϵ_1 at $q = 0$ for low frequency are therefore somewhat more uncertain than the low-frequency dielectric constants we report at finite wave vectors.

The maximum conductivity for $q = 0$ is seen to move toward higher frequency with increasing randomness. The reason for this is again the decrease in decay length, as we discussed in Sec. IV C. In comparison with Eq. (4.15), we find

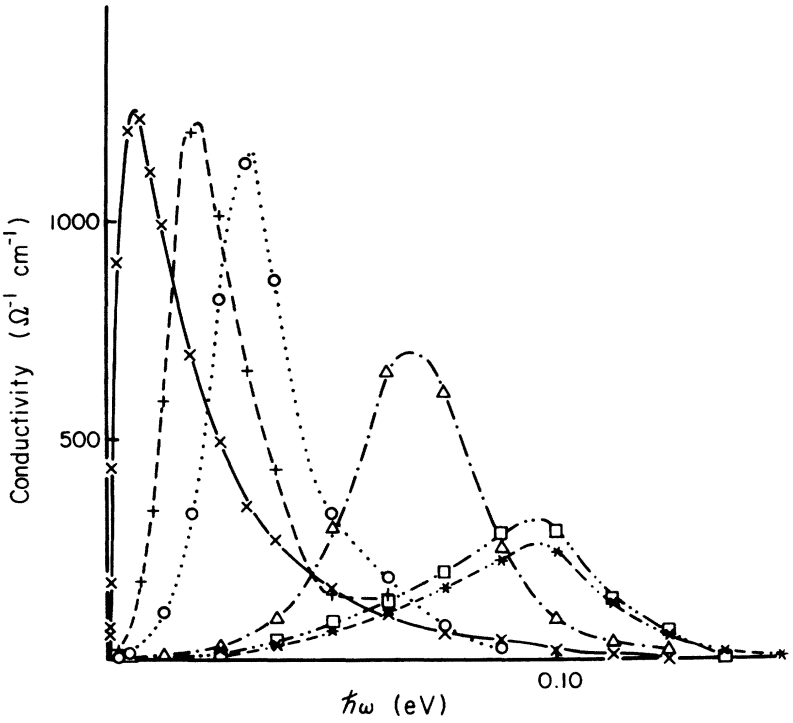

FIG. 15. Conductivity vs frequency for randomness 1.0. ×, $q=0.0$; +, $q=0.125\ \pi/b$; circles, $q=0.20\ \pi/b$; triangles, $0.50\ \pi/b$; squares, $0.90\ \pi/b$; asterisks, $1.00\ \pi/b$.

$\pi t/L = 0.0085$ eV for $S=1$, in fair agreement with the observed peak position at 0.0065 eV; for $S=1.5$, we have $\pi t/L = 0.0176$ eV, compared with the observed peak at 0.0140 eV. Both of these results are consistent with $\hbar\omega_{max} = 0.78\ \pi t/L$.

Although our theory predicts an ω^{-2} dependence for the conductivity at high frequencies, our data do not clearly show this behavior. At randomness 1 the drop in conductivity at large frequencies is considerably faster than $1/\omega^2$, while that for $S=1.5$ is slightly slower than the predicted rate. At these large frequencies the number of available states with energy difference sufficiently large is decreasing rapidly, since both initial and final states [k and k' in Eq. (4.13)] are in the tails of the band. This rapid decrease in densities of states is reflected in the high-frequency behavior of σ for $S=1$. For $S=1.5$, however, the decrease in the density of states is less rapid, resulting in behavior more like the $1/\omega^2$ expected for a constant density of states.

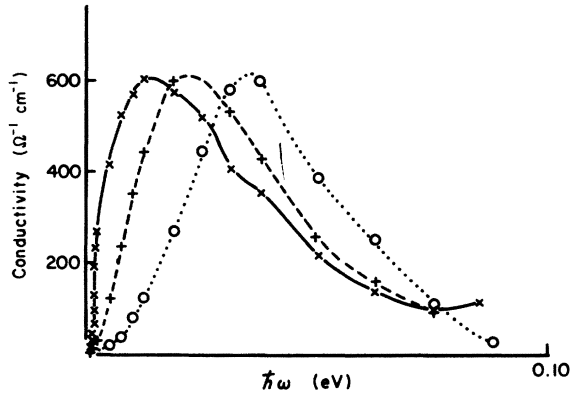

FIG. 16. Conductivity vs frequency for randomness 1.5. ×, $q=0.0$; +, $q=0.10\ \pi/b$; circles, $0.20\ \pi/b$.

There are a number of directions in which future research on this topic should go. First the variation with band filling should be investigated. Further it would be interesting to study variations with temperature, to add the effect of phonons, and to add electron-electron correlations.

ACKNOWLEDGMENTS

I should like to express my appreciation to Professor Morrel H. Cohen for his guidance throughout this project. In addition, I acknowledge discussions with Dr. T. P. Eggarter, and Dr. C. T. Papatriantafillou.

APPENDIX

We wish to show that the P_s converge to the values predicted for them in Eq. (5.29). We begin with P_0, which satisfies (5.25):

$$P_0(\phi, \phi', n+1) = \iiint d\epsilon\, d\phi_1\, d\phi_1'\, h(\epsilon) \times \delta(\tan^{-1}(E-\epsilon-\tan\phi_1)^{-1} - \phi) \times \delta(\tan^{-1}(E'-\epsilon-\tan\phi_1')^{-1} - \phi') P_0(\phi_1, \phi_1', n)\,, \tag{A1}$$

We wish to show that one is a nondegenerate eigenvalue of this kernel; and that all other eigenvalues are smaller in magnitude than one. If this is true, then $P_0(\phi, \phi', n)$ will converge to $p_0(\phi, \phi')$, where p_0 is the eigenvector of the kernel of (A1) belonging to the eigenvalue 1. [This can be seen by an expansion of $P_0(\phi, \phi', n)$ in eigenvectors of the kernel. If this expansion is iterated m steps farther, the jth term is multiplied by λ_j^m, where λ_j is the jth eigenvalue. In the limit $m \to \infty$ $\lambda_j^m \to 0$ unless $|\lambda_j| \geq 1$. Since we only have one eigenvalue 1, only its eigenvector (properly normalized) remains.]

To prove this we need one theorem from the mathematics of integral equations: If a kernel is bounded, both it and its transpose have the same eigenvalues with the same degeneracy[28] (but not, of course, the same eigenvectors). The kernel we have is not bounded, since it contains two δ functions and but one integral. The quantity

$$K_2(\phi, \phi'; \phi_1, \phi_1') = \int d\phi_2\, d\phi_2' \times K(\phi, \phi'; \phi_2, \phi_2') K(\phi_2, \phi_2'; \phi_1, \phi_1') \tag{A2}$$

is bounded except for the line $\phi = \phi' = 0$, $\tan\phi_1' = E' - E + \tan\phi_1$, and the quantity

$$K_3(\phi, \phi'; \phi_1, \phi_1') = \int d\phi_3\, d\phi_3' K(\phi, \phi'; \phi_3, \phi_3') \times K_2(\phi_3, \phi_3'; \phi_1, \phi_1') \tag{A3}$$

is bounded for all ϕ, ϕ', ϕ_1, and ϕ_1' as long as $h(\epsilon)$ is bounded. [This excludes from the possible distribution functions $h(\epsilon)$ such things as binary alloy distribution since they are unbounded. We may of course approximate any such δ-function distribution by one which is bounded but with a finite width.]

We may rewrite K_3 as

$$K_3(\phi, \phi'; \phi_1, \phi_1') = \int d\epsilon_1\, d\epsilon_2\, d\epsilon_3\, h(\epsilon_1) h(\epsilon_2) h(\epsilon_3)\, \delta(\tan^{-1}\{E - \epsilon_3 - [E - \epsilon_2 - (E - \epsilon_1 - \tan\phi_1)^{-1}]^{-1}\}^{-1} - \phi) \times \delta(\tan^{-1}\{E' - \epsilon_3 - [E' - \epsilon_2 - (E' - \epsilon_1 - \tan\phi_1')^{-1}]^{-1}\}^{-1} - \phi'). \tag{A4}$$

We observe first that

$$\int K_3(\phi, \phi'; \phi_1, \phi_1')\, d\phi\, d\phi' = 1\,. \tag{A5}$$

Thus the kernel which is the transpose of K_3 has one as an eigenvalue with the constant function as its eigenvector. Now let $\psi(\phi, \phi')$ by any eigenvector, and let λ be its eigenvalue. Further let $(\phi, \phi')_m$ be a point for which $|\psi(\phi, \phi')_m| \geq |\psi(\phi, \phi')|$. Thus we have

$$\lambda\psi(\phi_1, \phi_1') = \int K_3(\phi, \phi'; \phi_1, \phi_1')\, \psi(\phi, \phi')\, d\phi\, d\phi',$$

$$|\lambda\psi(\phi_1, \phi_1')| \leq \left|\int K_3(\phi, \phi'; \phi_1, \phi_1')\, d\phi\, d\phi'\right| |\psi(\phi, \phi')_m|\,, \tag{A6}$$

or

$$|\lambda|\, |\psi(\phi_1, \phi_1')| \leq |\psi(\phi, \phi')_m|\,.$$

Since this must be true for all (ϕ_1, ϕ_1') including $(\phi, \phi')_m$, we have $|\lambda| \leq 1$; and the equality can hold only if $\psi(\phi, \phi') = \psi(\phi, \phi')_m$ everywhere, i.e., if ψ is a constant. We have proved therefore that the kernel (transpose of K_3) has a nondegenerate eigenvalue 1, and hence K_3 must also have such an eigenvalue. Hence, by the argument following (A1), $P_0(\phi, \phi', n)$, converges to a value independent of n.

Alternatively, we might note that K satisfies the conditions of case b on p. 197 of Doob,[47] with X the square $-\frac{1}{2}\pi \leq \phi \leq \frac{1}{2}\pi$, $-\frac{1}{2}\pi \leq \phi' \leq \frac{1}{2}\pi$, $C = X$, $\phi = \pi^{-2}$, and $\nu = 3$. [That is, the probability of getting from any ϕ, ϕ' to any other in three steps is bounded below by a positive number. From this it follows that $P_0(\phi, \phi', n)$ converges to a quantity $p_0(\phi, \phi')$ independent of n or of the initial conditions.]

$P_1(\phi, \phi', n)$ also converges to a value independent of n for large n.[48] P_1 satisfies Eq. (5.26):

$$P_1(\phi, \phi', n+1) = e^{i\vec{q}\cdot\vec{b}} \sin\phi\, \sin\phi'\, P_0(\phi, \phi', n+1) + e^{i\vec{q}\cdot\vec{b}} (\cos\phi \cos\phi' \tan\phi \tan\phi') \iint d\phi_1\, d\phi_1'\, d\epsilon\, h(\epsilon) \times \delta(\tan^{-1}(E - \epsilon - \tan\phi_1)^{-1} - \phi)\, \delta(\tan^{-1}(E' - \epsilon - \tan\phi_1')^{-1} - \phi')\, (\cos\phi_1 \cos\phi_1')^{-1} P_1(\phi_1, \phi_1', n)\,. \tag{A7}$$

Because of the term in P_0 here, this case must be treated differently from the previous one. What we must show is that all eigenvalues of the kernel which overlap with P_1 are less than one in magnitude. From this it follows (by expanding P_0 in eigenfunctions of this kernel) that P_1 takes on the

limiting form

$$P_1=\sum_j(1-\lambda_j)^{-1}P_{0j}\psi_j(\phi,\phi'), \tag{A8}$$

where the sum is over all eigenvalues λ_j; ψ_j is the eigenfunction belonging to the jth eigenvalue, and P_{0j} is a coefficient in

$$P_0(\phi,\phi')\sin\phi\sin\phi' e^{i\vec{q}\cdot\vec{b}}=\sum_j P_{0j}\psi_j(\phi,\phi').$$

This limiting form is only valid if $|\lambda_j|<1$ for all j for which $P_{0j}\neq 0$. To show that the eigenvalues of this kernel are less than one, we exhibit a function Q which satisfies the same boundary conditions as P_1 at $n=2$ and which satisfies

$$\begin{aligned}Q(\phi,\phi',n+1)&=e^{i\vec{q}\cdot\vec{b}}(\cos\phi\cos\phi'\tan\phi\tan\phi')\\&\times\int d\phi_1\,d\phi_1'\,d\epsilon\,h(\epsilon)\,\delta(\tan^{-1}(E-\epsilon-\tan\phi_1)^{-1}-\phi)\\&\times\delta(\tan^{-1}(E'-\epsilon-\tan\phi_1')^{-1}-\phi')(\cos\phi_1\cos\phi_1')^{-1}\\&\times Q(\phi_1,\phi_1',n).\end{aligned} \tag{A9}$$

Because this is a first-order equation, there is only one such function. We show then that the function Q which satisfies the stated conditions must go to zero as $n\to\infty$. (Hence all the eigenvalues j of the kernel are less than one so that $\lambda_j^m\to 0$ as $m\to\infty$ for all j.)

We define

$$\begin{aligned}Q(\phi,\phi',n)=\cos\phi\cos\phi' e^{i\vec{q}\cdot\vec{b}(n-1)}\langle&[a_1(E)/a_n(E)]\\&\times[a_1(E')/a_n(E')]\,\delta(\tan^{-1}Z(n,E)-\phi)\\&\times\delta(\tan^{-1}Z(n,E')-\phi')\rangle.\end{aligned} \tag{A10}$$

By comparison with the definition of P_1 [Eq. (5.20)] we see that $P_1(\phi,\phi',2)=Q(\phi,\phi',2)$. Further, Q satisfies Eq. (A9).

We shall now show that $Q(\phi,\phi',n)\to 0$ as $n\to\infty$. We may reverse the argument of Eqs. (5.8) and (5.9) to write

$$\begin{aligned}Q(\phi,\phi',n)=e^{i\vec{q}\cdot\vec{b}(n-1)}\cos\phi\cos\phi'\Big\langle&\frac{a_1(E)}{a_n(E)}\,\frac{a_1(E')}{a_n(E')}\\&\times\left(\frac{\partial Z(n,E)}{\partial E}\right)^{-1}\sum_i\delta(E-E_i)\\&\times\left(\frac{\partial Z(n,E')}{\partial E'}\right)^{-1}\sum_{i'}\delta(E'-E_{i'})\Big\rangle,\end{aligned} \tag{A11}$$

where the E_i are eigenvalues of a chain of length $n-1$, with right-hand boundary conditions $z_R=\phi$; E_i' are similar energies with right-hand boundary condition $z_R=\phi'$. By Eqs. (5.5), (5.11), and (5.17) we observe that $(\partial Z/\partial E)^{-1}=-U^{-1}(E,n)=-a_n^2(E)$. Thus

$$\begin{aligned}Q(\phi,\phi',n)=\cos\phi\cos\phi' e^{iq\cdot b(n-1)}&\\\times\Big\langle a_1(E)a_n(E)a_1(E')a_n(E')\sum_i\delta(E-E_i)&\\\times\sum_{i'}\delta(E'-E_{i'})\Big\rangle.&\end{aligned} \tag{A12}$$

As $n\to\infty$, the δ functions, which are densities of states, increase as n. Because of the exponential localization of all states of a disordered one-dimensional Hamiltonian,[28] the product $a_1(E)a_n(E)$ is of order $e^{-n/L(E)}$, where $L(E)$ is the localization length at energy E.[29,30] [That is, a state has a maximum near site m, and decays exponentially on either side. Then we have $a_1(E)\sim e^{-m/L(E)}$ and $a_n(E)\sim e^{-(n-m)/L(E)}$, so the product is $a_1(E)a_n(E)\sim e^{-n/L(E)}$.] Thus we find $Q(\phi,\phi',n)\sim n^2\times e^{-n/L(E)-n/L(E')}$, which goes to zero as $n\to\infty$, and since

$$P_0(\phi,\phi',n)\to p_0(\phi,\phi'),\quad P_1(\phi,\phi',n)\to p_1(\phi,\phi')$$

as well.

We show, finally, that $P_2(\phi,\phi',n)\propto n$ for large n, but becomes independent of ϕ and ϕ'. [Given the way in which P_2 enters the formalism for $\epsilon(q,\omega)$, this is the only reasonable dependence, for it makes ϵ independent of the size of the material and the choice of boundary conditions.] To show this dependence we begin from Eq. (5.27):

$$\begin{aligned}P_2(\phi,\phi',n+1)=\int d\phi_1\,d\phi_1'\,d\epsilon\,h(\epsilon)\,\delta(\phi_1-\tan^{-1}(E-\epsilon-1/\tan\phi))&\\\times\delta(\phi_1'-\tan^{-1}(E'-\epsilon-1/\tan\phi'))[P_2(\phi_1,\phi_1',n)&\\+2\cos\phi_1\cos\phi_1'\,\mathrm{Re}P_1(\phi_1,\phi_1',n)+\cos^2\phi_1\cos^2\phi_1'P_0(\phi_1,\phi_1',n)].&\end{aligned} \tag{A13}$$

We note immediately that the kernel $K(\phi,\phi';\phi_1,\phi_1')$ in Eq. (A13) has the following properties: (a)

$$\int d\phi_1\,d\phi_1'K(\phi,\phi';\phi_1,\phi_1')=1. \tag{A14}$$

From this it follows [as in Eqs. (A5) and (A6)], that: (b) one is a nondegenerate eigenvalue of K; it is the largest eigenvalue in magnitude. (c) The eigenfunction belonging to this eigenvalue is a constant, independent of ϕ and ϕ'. We see then that this largest eigenvalue of K contributes $n\times C$,

where C is the coefficient of the constant term in the eigenfunction expansion of the inhomogeneous terms. The other eigenvalues contribute terms of the form

$$(1-\lambda_j)^{-1} D_j \psi_j(\phi, \phi').$$

As $n \to \infty$ these last mentioned terms become less and less important compared to the former, and $P_2 \to nC$.

To evaluate C, we must expand the inhomogeneous terms on the right-hand side of Eq. (A12) (the terms in p_0 and p_1) in terms of eigenfunctions of the kernel and retain the coefficient of the constant eigenfunction. That coefficient is $\psi_0^* \times$(inhomogeneous terms), where ψ_0^* is the adjoint function to ψ_0—the function which satisfies the homogeneous integral equation with the kernel transposed. It is easy to check that this function is $p_0(\tan^{-1}(1/\tan\phi), \tan^{-1}(1/\tan\phi'))$. Thus we have

$$C = \int d\phi\, d\phi'\, p_0(\tan^{-1}(1/\tan\phi), \tan^{-1}(1/\tan\phi')) \int d\epsilon\, h(\epsilon) \times \left(\frac{2\,\mathrm{Re} p_1(\tan^{-1}(E-\epsilon-1/\tan\phi), \tan^{-1}(E'-\epsilon-1/\tan\phi'))}{[1+(E-\epsilon-1/\tan\phi)^2]^{1/2}[1+(E'-\epsilon-1/\tan\phi')^2]^{1/2}} + \frac{p_0(\tan^{-1}(E-\epsilon-1/\tan\phi), \tan^{-1}(E'-\epsilon-1/\tan\phi'))}{[1+(E-\epsilon-1/\tan\phi)^2][1+(E'-\epsilon-1/\tan\phi')^2]} \right). \tag{A15}$$

Now define new variables ξ and η by $\tan\xi = E-\epsilon-1/\tan\phi$, $\tan\eta = E'-\epsilon-1/\tan\phi'$. In terms of these variables we may write

$$C = \int \frac{d\xi\, d\eta\, d\epsilon\, h(\epsilon)(\tan^2\xi+1)(\tan^2\eta+1) p_0(\tan^{-1}(E-\epsilon-\tan\xi), \tan^{-1}(E'-\epsilon-\tan\eta))}{[1+(E-\epsilon-\tan\xi)^2][1+(E'-\epsilon-\tan\eta)^2]} \times [2\cos\xi\cos\eta\,\mathrm{Re} p_1(\xi,\eta) + \cos^2\xi\cos^2\eta\, p_0(\xi,\eta)]. \tag{A16}$$

The integral over ϵ in Eq. (A16) may be done easily, using Eq. (5.15). With this transformation, Eq. (A16) becomes Eq. (5.30).

*Research supported by Army Research Office (Durham). We have also benefited from support of the Materials Research Laboratory of the NSF at the University of Chicago, and from a NSF Graduate Fellowship (1971–1974).

†Submitted in partial fulfillment of the requirements for a Ph. D. degree in the Department of Physics, The University of Chicago.

§Present address.

‖Radiation Laboratory is operated by the University of Notre Dame under contract with the ERDA. This is ERDA document number COO-38-991.

[1] M. J. Minot and J. H. Perlstein, Phys. Rev. Lett. 26, 371 (1971).

[2] D. Kuse and H. R. Zeller, Phys. Rev. Lett. 27, 1060 (1971).

[3] R. G. Kepler *et al.*, Phys. Rev. Lett. 5, 503 (1960).

[4] W. J. Siemons *et al.*, J. Chem. Phys. 39, 3523 (1963).

[5] I. F. Shchegolev, Phys. Status Solidi A 12, 9 (1972), and references therein.

[6] A. J. Epstein, S. Etemad, A. F. Garito, and A. J. Heeger, Phys. Rev. B 5, 952 (1972), and references therein.

[7] M. J. Rice and J. Bernasconi, Phys. Lett. A 38, 277 (1972); J. Phys. F 2, 905 (1972).

[8] M. J. Rice and J. Bernasconi, Phys. Rev. Lett. 29, 113 (1972).

[9] A. S. Berenblyum *et al.*, Zh. Eksp. Teor. Fiz. Pis'ma Red. 13, 619 (1971) [JETP Lett. 13, 440 (1971)].

[10] A. N. Bloch, R. B. Weisman, and C. M. Varma, Phys. Rev. Lett. 28, 753 (1972).

[11] Calculated from charge densities supplied by A. N. Bloch (private communication).

[12] C. J. Fritchie, Acta Crystallogr. 20, 892 (1966).

[13] H. Kobayashi, Bull. Chem. Soc. Jpn. 48, 1373 (1975).

[14] B. Morosin, Phys. Lett. A 53, 455 (1975).

[15] G. Theodorou and Morrel H. Cohen (private communication).

[16] H. Deiseroth and H. Schulz, Phys. Rev. Lett. 33, 963 (1974).

[17] J. M. Williams, J. L. Petersen, H. M. Gerdes, and S. W. Peterson, Phys. Rev. Lett. 33, 1079 (1974).

[18] M. Pollak, Proc. R. Soc. Lond. A 325, 383 (1971).

[19] L. I. Buravov *et al.*, Zh. Eksp. Teor. Fiz. Pis'ma Red. 12, 142 (1970) [JETP Lett. 12, 99 (1970)]; see also Ref. 5.

[20] N. E. Hill *et al.*, *Dielectric Properties and Molecular Behavior* (Van Nostrand, New York, 1969), pp. 232–240.

[21] K. G. Denbigh, Trans. Faraday Soc. 36, 936 (1940).

[22] A. I. Vogel *et al.*, J. Chem. Soc. 1952, 514.

[23] C. G. LeFevre and R. J. W. LeFevre, Rev. Pure Appl. Chem. 5, 261 (1955).

[24] J. Hurley and R. J. W. LeFevre, J. Chem. Soc. B 1967, 824.

[25] C. Kittel, *Introduction to Solid State Physics* (Wiley, New York, 1966), Chaps. 5 and 6.

[26] S. Etemad, A. F. Garito, and A. J. Heeger, Phys. Lett. A 40, 45 (1972).

[27] R. L. Bush, Phys. Rev. B 12, 5968 (1975).

[28] R. E. Borland, Proc. R. Soc. Lond. A 274, 529 (1963).

[29] C. T. Papatriantafillou, Phys. Rev. B 7, 5386 (1973).

[30] R. L. Bush, Phys. Rev. B 6, 1182 (1972).

[31] Morrel H. Cohen (private communication). The ϵ_n also have a Gaussian correlation for different n, which we ignore here.

[32]See, e.g., H. Ehrenreich and Morrel H. Cohen, Phys. Rev. 115, 786 (1959). Our Eq. (3.4) is their Eq. (10) without the assumption of plane waves as eigenstates.
[33]V. L. Berezinskii, Zh. Eksp. Teor. Fiz. 65, 1251 (1973) [Sov. Phys.-JETP 38, 620 (1974)].
[34]N. F. Mott and E. A. Davis, *Electronic Processes in Non-Crystalline Solids* (Clarendon, Oxford, 1971), p. 14.
[35]B. I. Halperin, Phys. Rev. A 139, 104 (1965); especially Secs. 2–4.
[36]R. Varga, *Matrix Iterative Analysis* (Prentice-Hall, Englewood Cliffs, N. J., 1962).
[37]E. Wachspress, *Iterative Solution of Elliptic Systems* (Prentice-Hall, Englewood Cliffs, N. J., 1966).
[38]A. C. Aitken, Proc. R. Soc. Edin. 46, 289 (1926).
[39]P. Wynn, Math. Comput. 16, 301 (1962); *Information Processing* 1962; *Proceedings of the International Federation for Information Processing Congress* 62, edited by C. M. Popplewell (North-Holland, Amsterdam, 1963), p. 149; Numer. Math. 6, 22 (1964).
[40]P. F. Williams and A. N. Bloch, Phys. Rev. B 10, 1097 (1974).
[41]J. Stuke, J. Non-Cryst. Solids 4, 1 (1970).
[42]R. E. Peierls, *Quantum Theory of Solids* (Oxford U.P., London, 1955), p. 108.
[43]M. J. Rice and S. Strässler, Solid State Commun. 13, 125 (1973).
[44]G. Theodorou and Morrel H. Cohen, Bull. Am. Phys. Soc. 20, 415 (1975).
[45]P. N. Sen and C. M. Varma, Solid State Commun. 15, 1905 (1974).
[46]A. N. Bloch (private communication).
[47]J. L. Doob, *Stochastic Processes* (Wiley, New York, 1953), p. 197.
[48]This argument and the argument for $P_2(n)$ at large n are based on those given by Halperin (Ref. 35).